OPEN ACCESS

ISSN: 2835-7868

Theilen-Willige B (2025): 424
J Earth Envi Sci, 2025; 4(2):100137
DOI: 10.71010/JEES.2025-e137

Research Article

Journal of Earth & Environment Science

Traces of Drifting and Rifting Processes in Central Egypt visible on different Satellite Images and on DEM derived morphometric Maps

Prof.Dr.habil. Barbara Theilen-Willige*

Retired from TU Berlin, Institute of Applied Geosciences, Waldstrasse 11 a, 23683 Scharbeutz, Germany

***Corresponding author:** Barbara Theilen-Willige, Email: Barbara.Theilen-Willige@t-online.de

Citation: Theilen-Willige B (2025) Traces of Drifting and Rifting Processes in Central Egypt visible on different Satellite Images and on DEM derived morphometric Maps. J Earth Envi Sci: JEES-137.

Received Date: 20 May, 2025; **Accepted Date:** 28 May, 2025; **Published Date:** 03 June, 2025

Abstract

In the scope of this study the detection of the structural-geologic pattern in Central Egypt was carried out based on different open-source satellite data (Landsat, ASTER, Sentinel 2, Sentinel 1 and ALOS PALSAR radar data), as well as on Orbview3, Google Earth and Bing Map high resolution satellite images. Some of the structural and lithologic features seem to trace rifting and gliding processes, especially along the N-S oriented Kharga valley and at the western and southwestern margin of the Sinn el Kaddab plateau. Circular and oval-shaped structures, obviously related to rotation, and block-wise movements of dislocated blocks could be observed on the different satellite images. Morphometric maps and indicators derived from Digital Elevation Model (DEM) data supported the detection of neotectonic deformations and of mass movements along the borders of the Sinn el Kaddab plateau. Because of these traces of intense geodynamic and geomechanically strain in this area the question arises, whether these traces are related to larger rifting processes along the Kharga valley and the SW border of the Sinn el Kaddab plateau or are just the result of block-wise uplifting of the Sinn el Kaddab plateau with different intensities, including isostatic and tectonic subsidence at the margins. Based on the gained knowledge by evaluations of remote sensing data areas for further, focused research with adapted geophysical methods could be pointed out.

Keywords: Rift zones; drifting; rotation; Central-Egypt; remote sensing; GIS

1. Introduction

Continental rifting is one of the major important geological processes on Earth. Rift basins are profound manifestation of intra-continental extensional tectonics [1] [2]. Extensional thinning and heating of the continental lithosphere during rifting leads to localized isostatic and tectonic subsidence and deposition of thick syn-rift sediments [3]. At the end of a given rifting episode, the crust/ upper mantle cools resulting in additional subsidence and accumulation of post-rift sediments.

Some examples of rift structures, which led to basins infilled with magmatic-sedimentary successions, include Central and Eastern Egypt [3] [4]. Several areas have been identified to have been prone to rifting such as the Gulf of Suez and the Red Sea, and the Nile valley [5] [6]. Several NW–SE-oriented Cretaceous intercontinental rift basins have been described in central and southern Egypt (Komombo, Nuqra and Kharit basins, Figure 1). The rifting has been accommodated by vertical extensional displacement on preexisting faults forming complex arrays of half-grabens and asymmetric horsts. Extensional displacement often occurred along preexisting faults [6] [7].

The area of interest is situated along the western and south-western border of the Sinn El Kaddab plateau, comprising parts of the Kharga valley, the Western Desert and the Nubian plane (Figure 1). As traces of intense geodynamic and geomechanical strain have been detected in this area in previous works such as rotational structures or dislocated blocks [8] [9] [10] [11], the question arises, whether these traces are related to larger rifting processes or just the result of uplifting of the Sinn el Kaddab plateau.

Most intraplate faults formed during previous tectonic settings when the stress regime was likely different. Recognition of multiple episodes of superposed intraplate deformation is extremely difficult, if not altogether impossible when later deformation has overprinted the signature of earlier tectonic episodes. The result is a complex array of various intraplate structural domains with varying degrees of deformation as the detailed tectonic evolution of individual intra-continental areas largely depended on their orientations/positions in relation to the stress generating orogenic processes at the continental margin [12]. This might be the case in the study area as well. Rift-related reactivation of Paleozoic faults and corresponding inheritance even for older structures was documented [13].

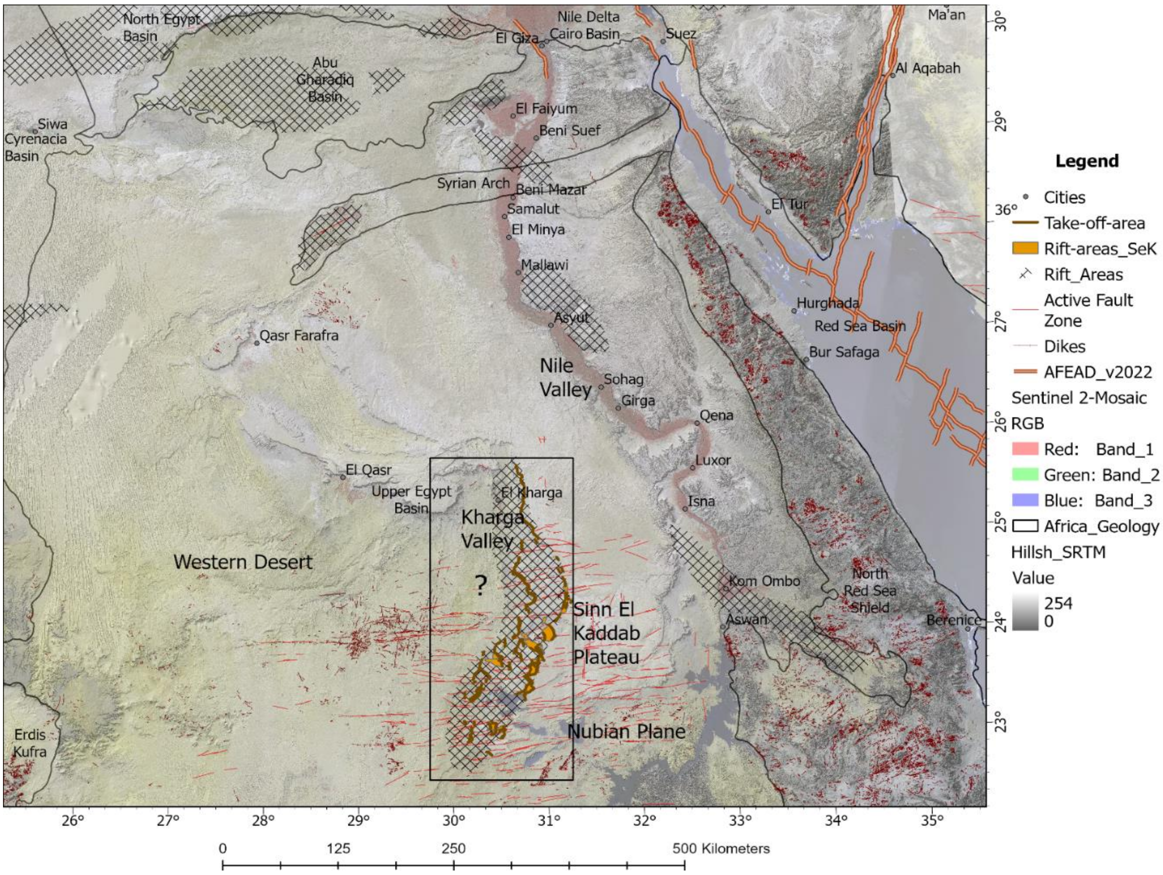

Figure 1: Overview of the major Mesozoic and Cenozoic land surface-rift basins in Egypt and position of the investigation area with an assumed rift zone (information about the rift areas: [1], [14], [4], the faults in the Red Sea: Active Faults of Eurasia Database (AFEAD) [15], Sentinel 2-image mosaic: [16].

A. *Aim of this Study*

More detailed investigations were carried out in the scope of this study based on satellite data, geodata, maps and references aiming to contribute to a more detailed structural knowledge: The systematic inventory of indicators such as the detection of rift valleys, dislocated blocks, rotation structures, etc., serving as basic data set, as well as the detection of traces of morphodynamic activities such as slope failure or relatively stronger erosion / sedimentation. The specific aim of this study is to investigate the structural pattern of the area in the west of the Sinn el Kaddab plateau, Western Desert and Kargha valley to gain information about traces of geodynamic activities, especially of traces of drifting and rifting.

Previous data evaluations have indicated already that a relative higher geodynamic activity including rifting processes is involved in the structural / tectonic development of this area [17], [9], [10],[11]. The question arises whether these traces (as listed below) are indicating the existence or even the development of a larger rift zone as presented in Figure 1 within the marked investigation area, or are they just the side effect of block-wise uplifting of the Sinn el Kaddab plateau with different intensities, including isostatic and tectonic subsidence at the margins? Some indicators and factors for drifting and rifting processes can be derived from evaluations of satellite data as summarized in Figure 2. They comprise:

- Traces of active fault zones and the fault pattern (as far as not covered by aeolian sediments),
- circular and oval shaped structures probably caused by rotation
- larger block movements of dislocated rock units,
- congruent borders between dislocated lithologic units, interrupted by valleys with traces of rift-valley development,
- morphometric indicators: steep slopes at the take-off zones, depressions at the backside of dislocated blocks due to mass deficits,
- intensity and frequency of mass movement and slope failure concentrated along take-off zones,
- intensity of visible morphodynamical processes such as linear erosion, sedimentation, alluvial fans, etc.,
- traces of past magmatic activity (dikes, plugs, craters) providing information about zones of weakness that might be reactivated again in the scope of recent geodynamic movements.

Of course, the evaluations of remote sensing data have to be verified as far as possible by combing the results with other geodata. For the documentation and monitoring of rifting and drifting processes data mining and the elaboration of a GIS data base is essential. Aiming to set up a GIS data base for this purpose and to integrate geophysical and other geodata into this GIS data base, the following data were processed:

- Geophysical data such as Bouguer gravity, magnetic anomalies, Curie Point Depth-CPD data, heat flow data

Information derived from measurements from mess stations:

- earthquake occurrence and concentrations

Goal is the delineation of faults, and the mapping of features associated with drifting and rifting of rock units that can help to improve the understanding of the geodynamic pattern in Central-Egypt.

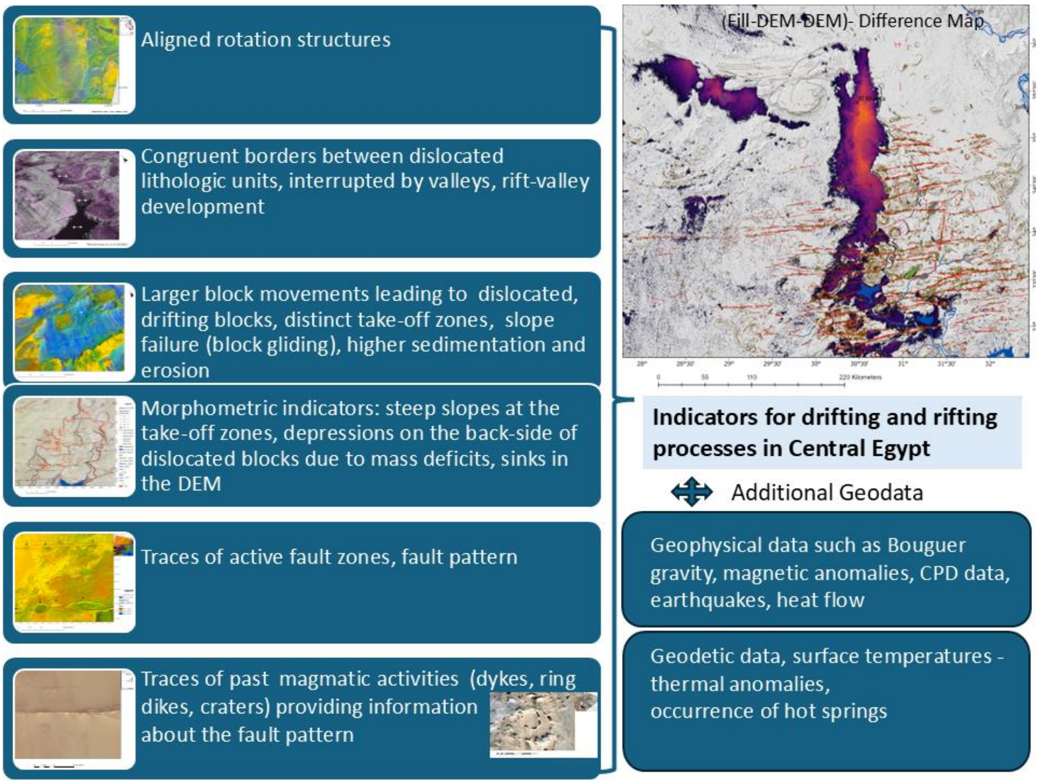

Figure 2: Detection and mapping of indicators for the occurrence of drifting and rifting processes based on remote sensing data and further available geodata.

2. Materials and Methods

In the scope of this study the structural analysis was carried out based on different open-source satellite data (Landsat, ASTER, Sentinel 2, Sentinel 1 and ALOS PALSAR radar data), as well as on OrbView3, Google Earth and Bing Map high resolution satellite images. Evaluations of different available geophysical data were integrated (Figure 3).

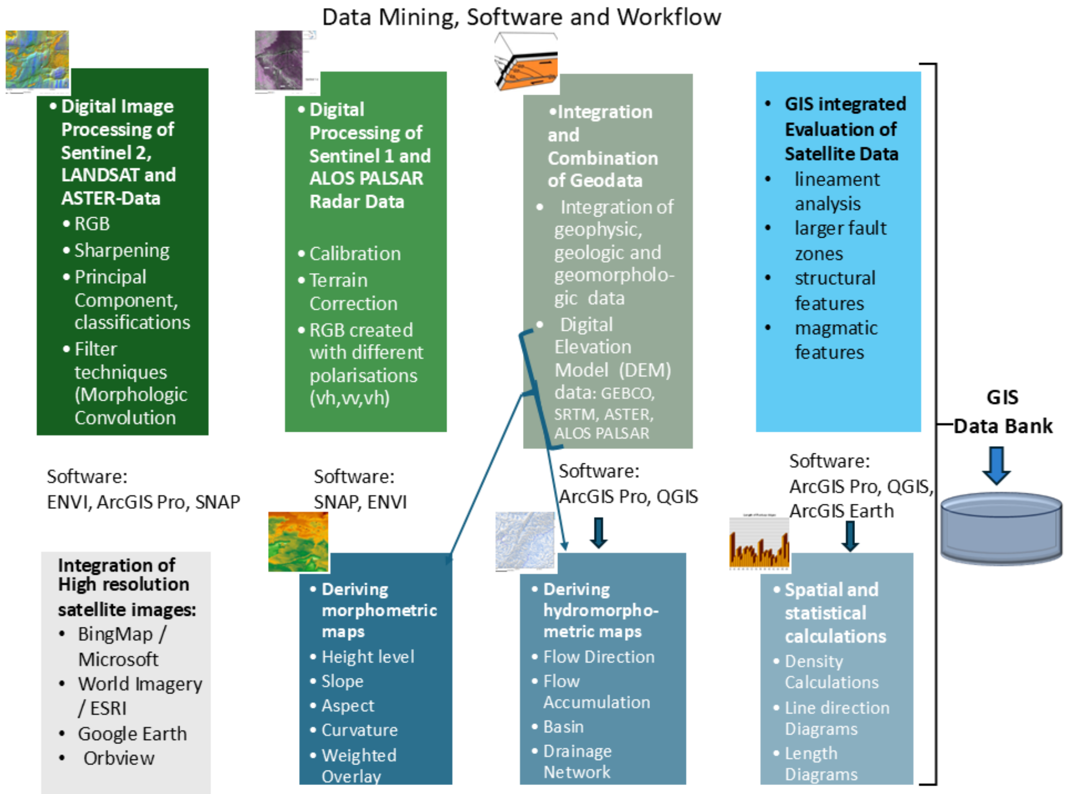

Figure 3: Satellite data, software, data processing and workflow [10] [11].

A. Evaluations of optical Satellite Data

The optical satellite data were provided by the USGS Earth Explorer [18], the ESA Copernicus Browser [19], and NASA Earth Data [20]. OrbView-3 satellite images from the investigation area were collected between 2003 and 2007 by Orbital Imaging Corporation (now GeoEye) at up to one-meter resolution. The OrbView-3 data set includes scenes of one meter resolution (panchromatic, black and white), and of four-meter resolution multi-spectral (color and infrared) data.

As digital image processing software served the Sentinel Application Platform (SNAP) / ESA and ENVI / NV5 Geospatial-Software as well as the processing tools integrated into the geoinformation systems ArcGIS Pro / ESRI and QGIS. The specific digital image processing methods such as the filter techniques of the different satellite data and image enhancements methods are focused on gaining additional knowledge about the structural pattern. Digital image processing of Orbview, Landsat TM 8 /9 (the Operational Land Imager (OLI), Sentinel 2 and ASTER (Advanced Spaceborne Thermal Emission Reflection Radiometer) data was carried out, mainly by merging different Red Green Blue (RGB) band combinations. Special attention was focused on the creation of RGB images of the Landsat 8 / 9 and ASTER thermal bands. Remotely sensed thermal-infrared imageries are generally used as base for estimates of land-surface temperatures that in this arid environment of Central-Egypt are related to lithologic and structural conditions.

B. Evaluation of Satellite Radar Images

The radar data were provided by the ESA Copernicus Browser [19], and NASA Earth Data, Alaska Satellite Facility (ASF) [20]. ALOS PALSAR mosaics) were retrieved from the Earth Observation Research Center, PALSAR global mosaic and Forest/Non-forest Map, JAXA [21]. The Advanced Land Observing Satellite (ALOS), Phased Array type L-band Synthetic Aperture Radar (PALSAR) from the Japan Aerospace Exploration Agency (JAXA) provided data with 12.5 m spatial resolution. The Sentinel 1 and ALOS PALSAR radar missions included dual polarization capabilities. By sending out radio waves that bounce off objects and return as echoes, radar creates a detailed picture of the surface. The radar system is able to transmit a signal in a horizontal (h) or vertical (v) polarization and receive in both h and v polarizations. RGB- tools were used here to merge radar images with different polarizations and, thus, get “false-colored” radar images improving the evaluation possibilities, for example by Sentinel 1-vh, vv, vh polarization composites. The different radar wavelengths correlated with the L-Band (23.5 cm) and C-Band (5.6 cm) allow varying radar penetration depths into the surface from a few centimeters up to meters. Sentinel 1 Synthetic Aperture Radar (SAR, C-Band, 5.6 cm wavelength), ALOS PALSAR (L-Band, 23.5 cm wavelength) radar data were digitally processed and evaluated. The processing of the radar data was carried out using the SNAP software of European Space Agency (ESA) and the image processing tools integrated in ArcGIS Pro /ESRI.

C. Evaluations of DEM Data

Morphometric maps and indicators derived from Digital Elevation Model (DEM) data support the detection of the neotectonic and morphodynamic processes. To automatically identify landform types, the relief elements are grouped into terrain features such as height levels, slope gradients, and terrain curvature. Morphometric maps such as slope, hillshade, height level, drainage, and slope maps were generated based on SRTM, ASTER GDEM [18] and ALOS PALSAR Digital Elevation Model (DEM) data [20] using ArcGIS Pro / ESRI and QGIS digital image processing software. The combination of structural and lithological data with morphometric indicators in a GIS environment is a methodological approach to identify traces of neotectonic movements and their resulting structures. From DEM (Digital Elevation Model) data derived morphometric maps were combined with lithologic and seismotectonic information in a GIS database.

D. Geophysical Data

The present study was carried out applying an integrated approach of processing and interpretation of both Bouguer gravity and aeromagnetic data, combined with available geological data to gain more structural information [22]. Using and combining information of heat flow, Bouguer gravity anomalies, magnetic anomalies, rock types, Moho depth, Lithosphere–Asthenosphere boundary depth, and depth to Curie point, supports the knowledge about the subsurface structures in the investigation area. Regions with a thinner crust and a shallower Moho tend to experience higher surface temperatures due to the increased thermal impact of the asthenosphere [24] [25]. The gravity field gives an integrated response to density contrasts caused by structural features on regional and local scales. Information of geothermal anomalies and global heat-flow data provided by the International Heat Flow Commission [23] were included as well, containing data generated between 1939 and 2024. Earthquake data were downloaded from USGS [26], EMSC [27] and ISC [28].

E. Structural Evaluations of satellite Images

Lineament analysis was an important part of this study. (The term lineament is a neutral term for all linear, rectilinear or slightly bended image elements.) Lineaments are often expressed as scarps, linear valleys, narrow depressions, linear zones of abundant watering, drainage network, peculiar vegetation, landscape and geologic anomalies. Linear arrangement of pixels depicting the same color / gray tone were mapped as linear features, as lineaments. They represent in many cases the surface expression of faults, fractures or lithologic discontinuities.

When evaluating the satellite data the following components were digitized:

- linear features – lineament analysis, analysing the orientation of linear segments and features using the Line Direction tool implanted in QGIS (rose diagrams).
- structural features (synclines, anticlines, active fault zones with pull-apart depressions and push-up-ridges, take off-areas, rift valleys, etc.). Distinct topographical features, including the formation of push-up ridges at restraining bends and deep pull-apart basins at releasing bends were digitized. As push-up ridges and pull-apart basins were mapped isolated, elongated inselbergs and depressions. As their internal structure (syncline, anticline, flower structure) often cannot derived from satellite data alone, especially the smaller ones, these terms are used in this context as a geomorphological description. Positive or negative height variations can be verified by comparisons of the high resolution satellite images with DEM data (Figure 4).

All these features were integrated into the GIS data base. Further on, density calculations of structural features were elaborated in ArcGIS Pro.

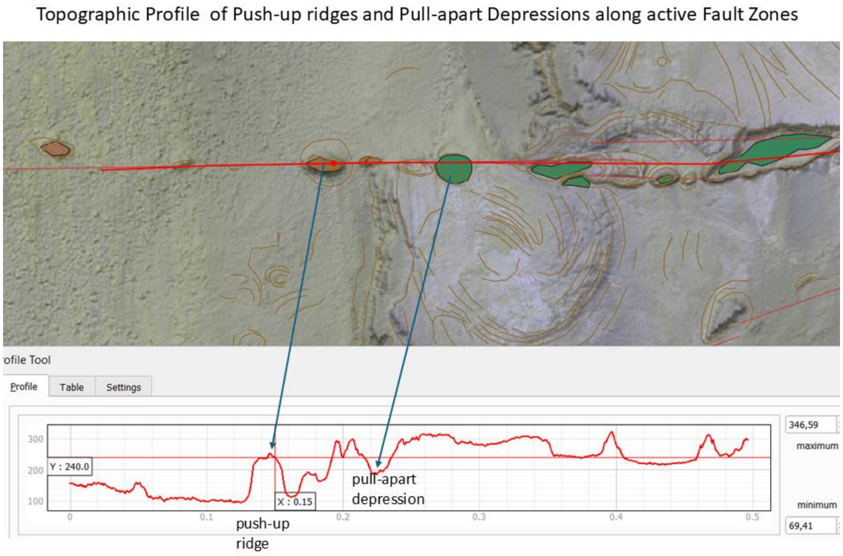

Figure 4: Morphologic description of push-up ridges and pull-apart depressions

3. Geographic and Geologic Setting

The investigation area comprises a variety of landforms including the Nile valley, the Sinn El-Kaddab limestone plateau, the Kharga valley, the Western Desert, the Nubian Plain, depressions with oases, large dune fields, playas, isolated hills, narrow ridges, often caused by dikes. Karst landforms are observed on the satellite images of the plateau region with height levels above 500 m due to the presence of the Eocene carbonate rocks. The Kharga valley and depression with height levels below 120 m is bounded to the north and east by distinct escarpments bordering the surrounding plateaus. The widespread Quaternary sediments display different formations such as aeolian sand sheets and dunes, and fluvial sediments accumulated even recently after now rare heavy rains in this arid environment. Traces of past magmatic activity form important parts of the landscape (dikes, craters) as well as traces of tectonic movements (cliffs, push-up-ridges, pull-apart depressions).

The African Eurasian plate boundary, the Red Sea plate margin and the Levant transform fault represent
Egypt's tectonic boundaries [29], [30]. The tectonic deformation mainly resulted from the interaction between the European and African plates which started in the Pre-Cambrian time and rejuvenated during the Hercynian (Pre-Carboniferous), Laramide (Late-Cretaceous) and Alpine (Late-Tertiary) orogeneses. Recent global positioning system observations reveal Africa's northwest ward movement relative to Eurasia at a rate of 6 mm per year. The Red Sea's spreading rates range from 14 mm per year to 5.6 mm per year [25].

The surface geological setup of Central-Egypt shows exposures of the Neoproterozoic (900–550 Ma) basement rocks dissected by intracratonic rift basins [14]. The basement was affected by various episodes of geodynamic activity and resulting faults; an older one with predominantly E-W and NW axes intersected by a younger N-E set of folds [30]. Reactivated basement structures play an important role in the structural pattern.

Due to the intense tectonic compressions from southeast to northwest and from east to west during the geologic past and even until recent times, fault structures control the tectonic framework of the study area, which is characterized by the superposition of the E-W- and N-S-trending compressive structures, by uplift and thrust in northern Egypt from Early Tertiary to Middle Eocene. Middle Tertiary appear a new regional extensional forces ENE-WSW resulted two complementary primary shear rifting system NW-SE (Red sea or Gulf of Suez trend) and NNE-SSW [22], [31].

The onset of the main rifting phase that controlled the evolution of the Nile Valley and its drainage was contemporaneous with the initiation of the Red Sea-Gulf of Suez and East African rift systems during the Oligocene ~30-28 Ma, and the concomitant regional uplifting processes, terrain exhumation and volcanism of the eastern Red Sea-Gulf of Suez hills [1]. Three main Late Paleogene-Early Neogene rift segments-trending NW and NNW can be characterized along the eastern and western shoulders of the river. These rift segments and their bounding faults were rejuvenated along NW- to NNW-oriented intracontinental half-graben basins that formed earlier during the Early Cretaceous rifting.

The Nubian Fault System (NFS) is extended from the Nile valley across the Western Desert. The NFS is composed of several E-W Principal Deformation Zones (PDZ) characterized by Late Cretaceous to present intra-plate strike-slip faults and related fold structures, as well as regional basement uplifts [32]. Little is known so far whether there might be rifting at the western border of the Sinn el Kaddab plateau.

4. Results

The derived results are subdivided according to their geomorphologic, geologic and geophysical features and expressions related to drifting and rifting processes.

A. *Traces of active fault zones*

A fault is considered active if there is evidence of distinctly visible displacements at the surface. Evidence for fault activity is whenever typical structural features such as pull-apart basins and depressions or push-up ridges along the fault occur. Another criterion is the evidence of displacement during the Holocene and the documentation of earthquakes along this fault zone as well as movements confirmed by geodetic surveys. Active faults play an important role for the development of drifting and rotation of rock units, especially along the E-W strike-slip fault zones, showing displacements, step-overs and deformations. These fault zones have been probably repeatedly active with a polycyclic motion history, including growth phases, and inactivity phases. This leads to complex and repeated reactivation of faults and fault segments resulting in complex, often lense-shaped structures and stratigraphy.

The type and character of movements along fault zones largely determines the dynamics of the typical structural features related to the fault zone (push-up ridges, pull-apart depressions, flower-structures) and of block movements. Examples are shown in the next figures (Figure 5 a and b) to demonstrate which fault zones were digitized based on different satellite images as active fault zones. SRTM DEM derived aspect maps support the detection of larger fault zones because of their distinct morphologic exposure.

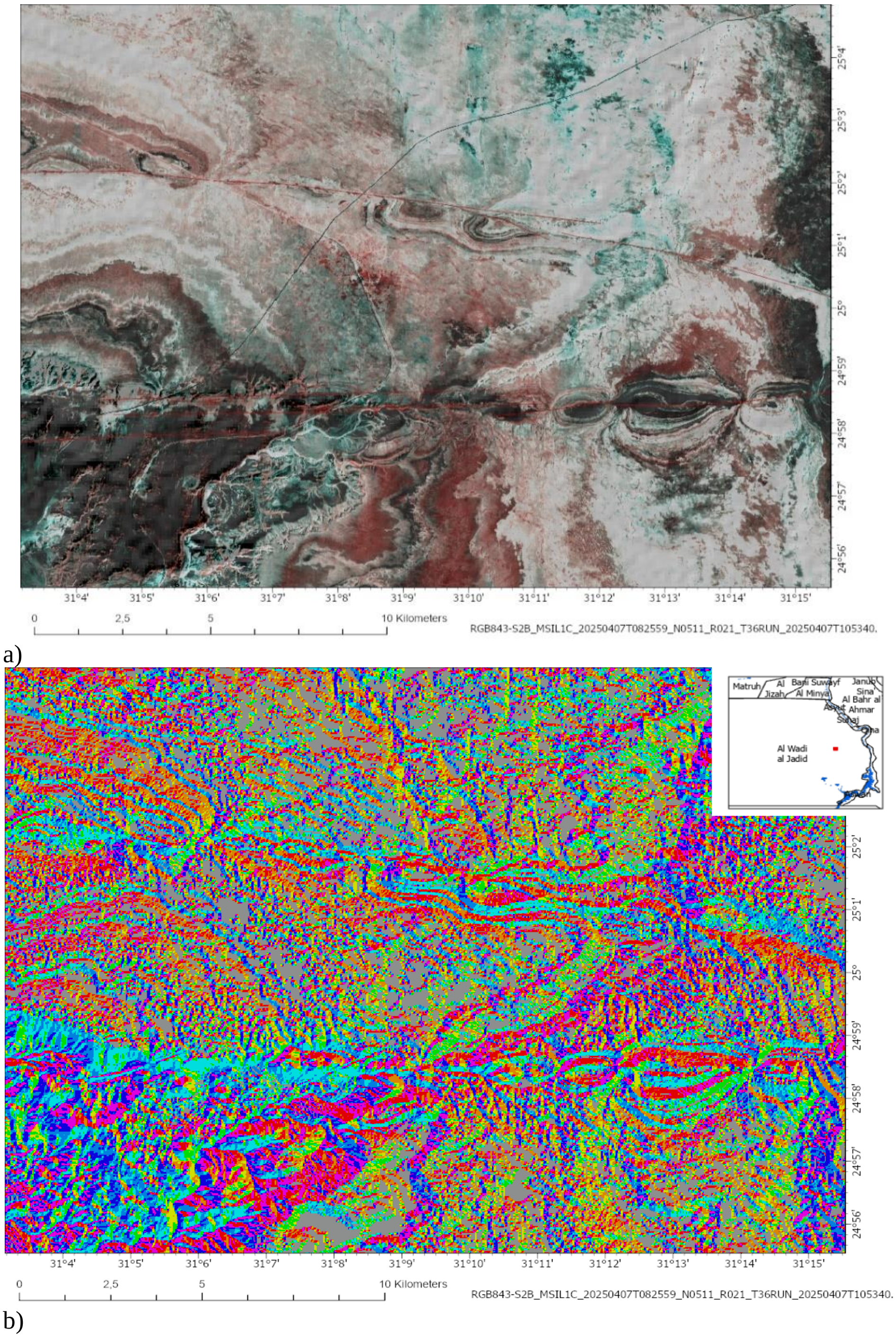

Figure 5 a and b: Sentinel 2-scene of active faults (red line; the black line in 5 a) shows a street) with fault related deformations and structures (a) and aspect map (SRTM DEM) of the same area (b). A fault with distinct deformation patterns like lense-shaped ridges is considered to be still active.

B. Rotation structures

Movements along larger fault zones with different vertical and horizontal sizes and orientations, velocities and intensities can initiate rotations of the rocks between them, especially whenever larger fault zones intersect each other. Several processes like uplift, chemical diagenesis and overpressure turn rocks into over materials that exhibit brittle or ductile behavior. Active faults are not only related to displacements of larger, horizontal block movements, but also have influenced rotation and rifting processes. It seems that both cases happened: a)

Larger rotation structures have been intersected and displaced by active fault zones. The rotation took place before the strike-slip faults occurred. b) The rotation was initiated and developed because of the fault movements.

The mapping of structural features based on the different satellite images reveals circular and oval structures surrounding the Sinn el Kaddab plateau. The circular and oval-shaped structures mainly occur within lithologic outcrops of Tertiary shales, marls, lime- and dolostones, or partly sandstones. Their morphological and structural pattern with multi-ringed, parallel and equidistant smaller ridges and valleys with height differences about 10 to 20 m seems to be related to rotation of "blocks" comprising the shales, marls and limestones (Figures 6, 7 and 8). Of course, other origins than rotation cannot be excluded without field verification such as up doming of the strata because of magmatic bodies in the subsurface or karst related dynamics. The latter are in general smaller features (about < 100 m) in this area.

The most prominent and largest structure is shown in Figure 7 (about 30 km width, 40 km length). Radar images and morphometric maps such as slope gradient and height level maps reveal its structural features.

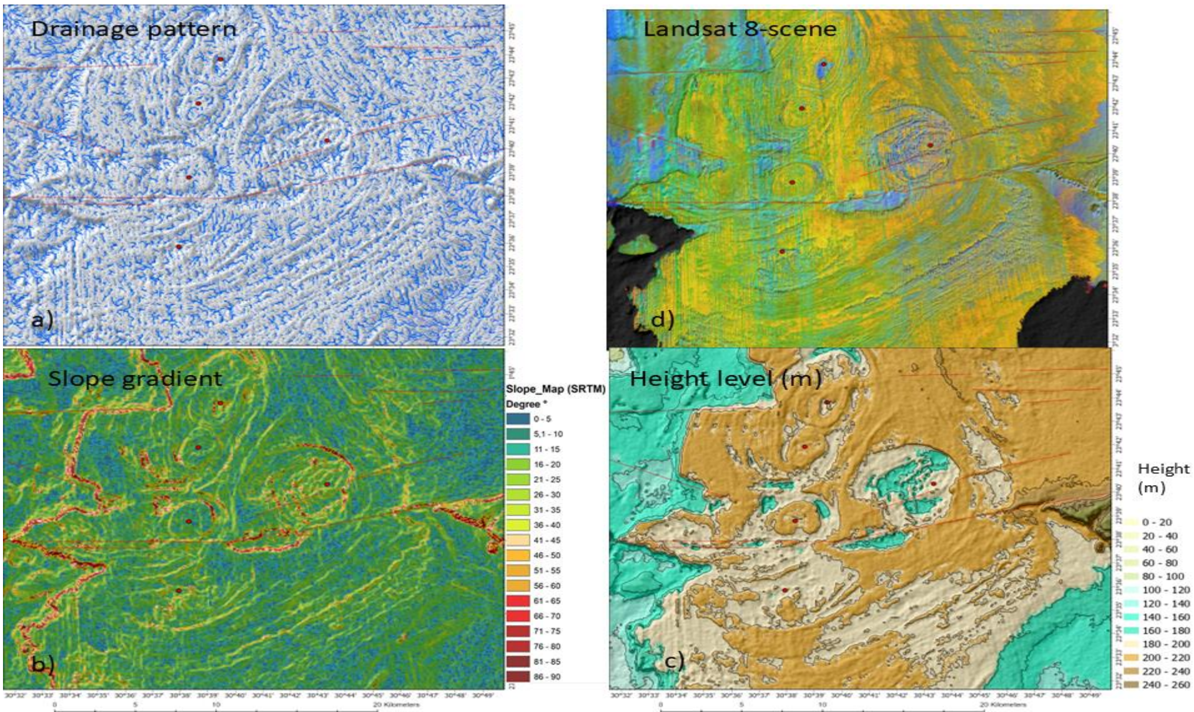

Figure 6: Circular and oval-shaped structures and their morphometric surface expression as visible on morphometric maps. (a) drainage pattern; (b) slope gradient; (c) height level; d) Landsat scene. Red lines represent traces of fault zones.

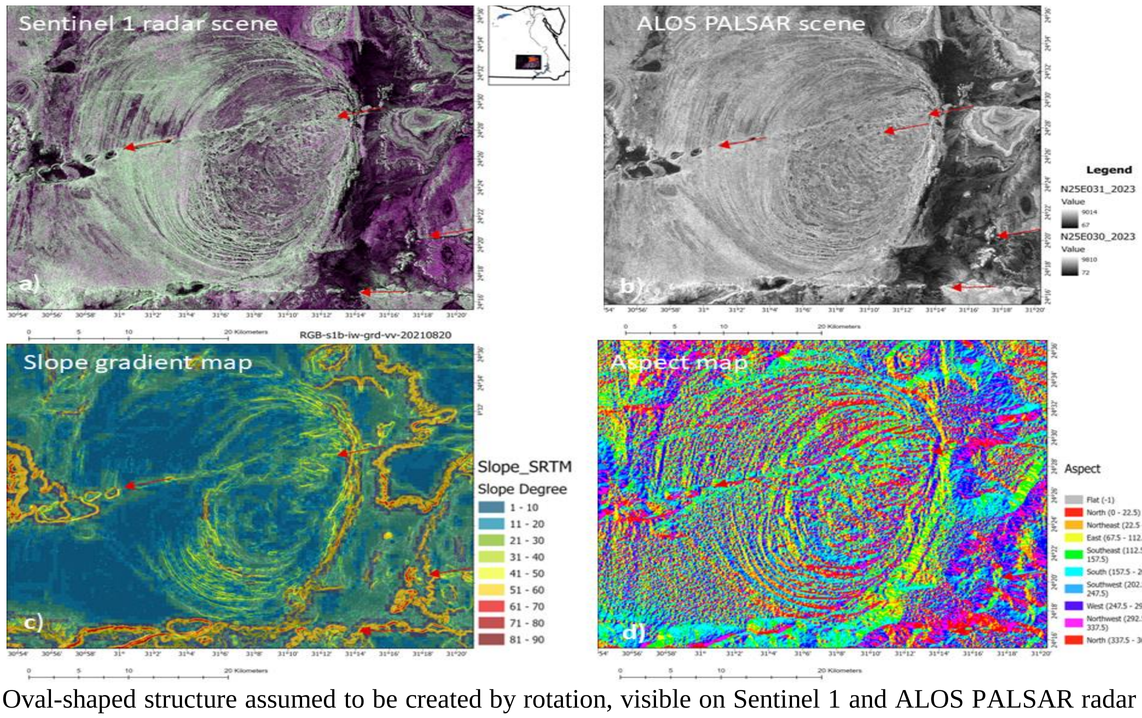

Figure 7: Oval-shaped structure assumed to be created by rotation, visible on Sentinel 1 and ALOS PALSAR radar images (a, b) and on SRTM DEM derived slope map and aspect map (c, d). The red arrows indicate larger, active fault zones with fault related push-up-ridges and pull-apart-depressions.

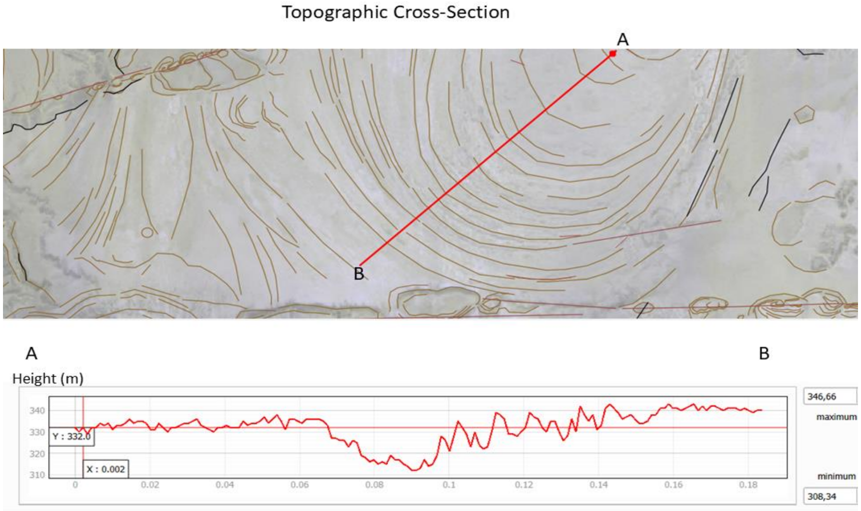

Figure 8: Topographic cross section along the oval-shaped structure indicating small sequences of ridges and depressions.

The dynamic of the assumed rotation processes was obviously influenced by movements along active fault zones and by vertical movements. Uplifting of the Sinn El Kaddab plateau might have contributed to rifting and rotation processes at its margins. The overlapping stress pattern caused by NW to NNW directed movements of the African plate and rifting of the Red Sea in the east might be a further, additional influencing factor.

The lithologic disposition of the host rocks played an important role as well. These circular structures with distinct surface expression are aligned along an approximately 50 km wide "belt" along the western Sinn el Kaddab Plateau and the Kharga valley in SSW-NNE direction. Their occurrence and frequencies are increasing from N to S, whereas the sizes of the circular structures are decreasing towards south. Based on the center points of the structures the density of their occurrence was calculated. The highest density of assumed smaller rotation structures can be observed in the SW of the Sinn el Kaddab plateau (Figure 9). Along the eastern border towards the Nile valley fewer, smaller and less pronounced, circular structures can be observed aligned in N-S and NNE-SSW direction.

C. Congruent Borders between dislocated lithologic Units interrupted by Valleys,

The next Figure 10 provides an example of a beginning rifting of Tertiary rock units, visible on a ALOS PALSAR radar scene. The SSW-NNE oriented valley at the western border of the Sinn el Kaddab Plateau shows that the contours of both sides of the valley correspond to each other. This valley is situated between different lithologic units: the Palaeocene units with prevailing marls and shales in the west and Eocene units with prevailing limestones in the east. The development of the valley was obviously initiated by movements along the horizontally moving (strike-slip) faults (see black arrows on Figure 10). Erosion was modelling the valley as well. The congruence of the valley rims, steep slopes along the take-off zones, the intense erosion and sedimentation along the eastern valley margins, support the assumption of rifting processes as well as the steep escarpment at the eastern flank, the flat bottom and the lower western flank (Figures 11 and 12). Deep seated fault zones in the basement, obviously repeatedly reactivated during the geologic past, still seem to have an influence on more recent geodynamics.

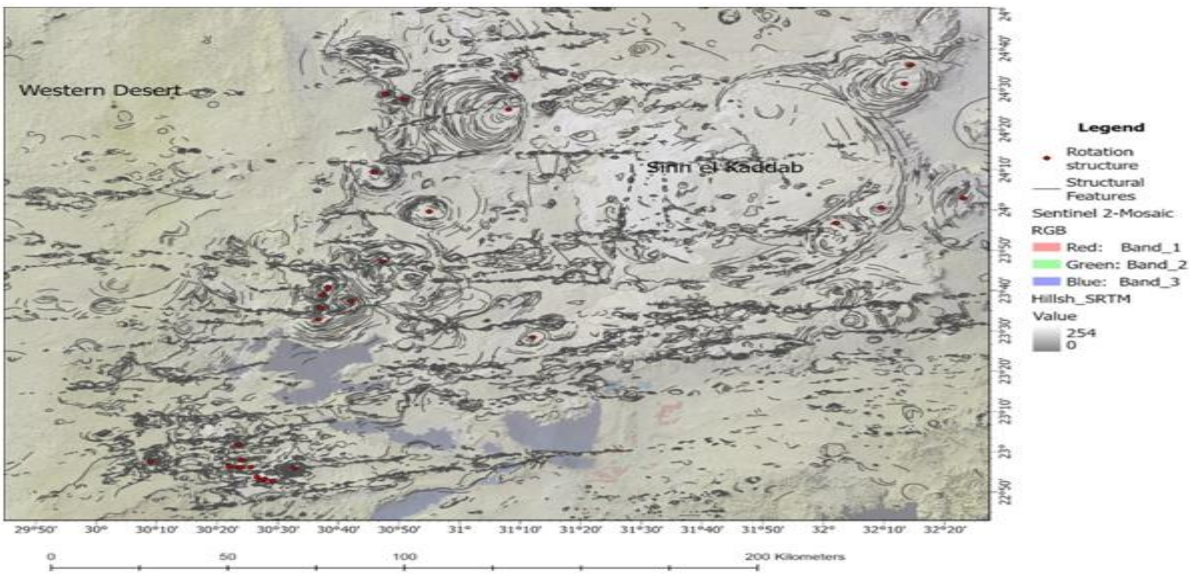

Figure 9 a: Circular and oval structures (red points at its centers) visible on the different satellite images, assumed to be created by rotation.

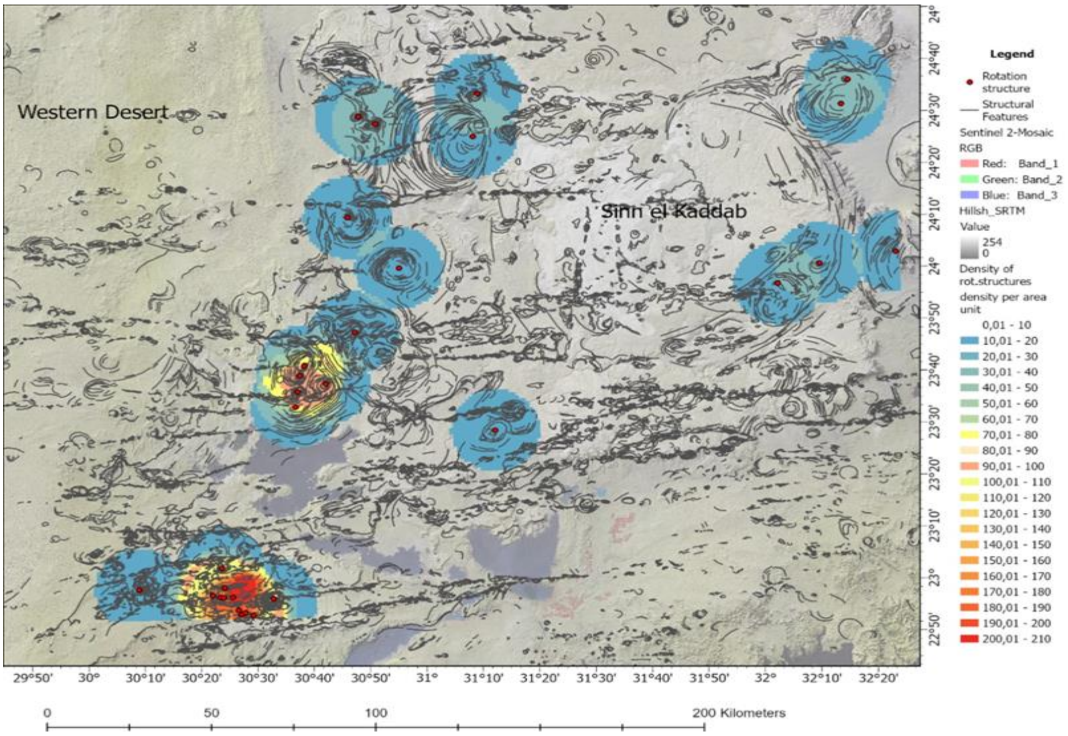

Figure 9 b: Density of circular structures assumed to be created by rotation aligned along a "belt" bordering the west and southwest of the Sinn el Kaddab plateau.

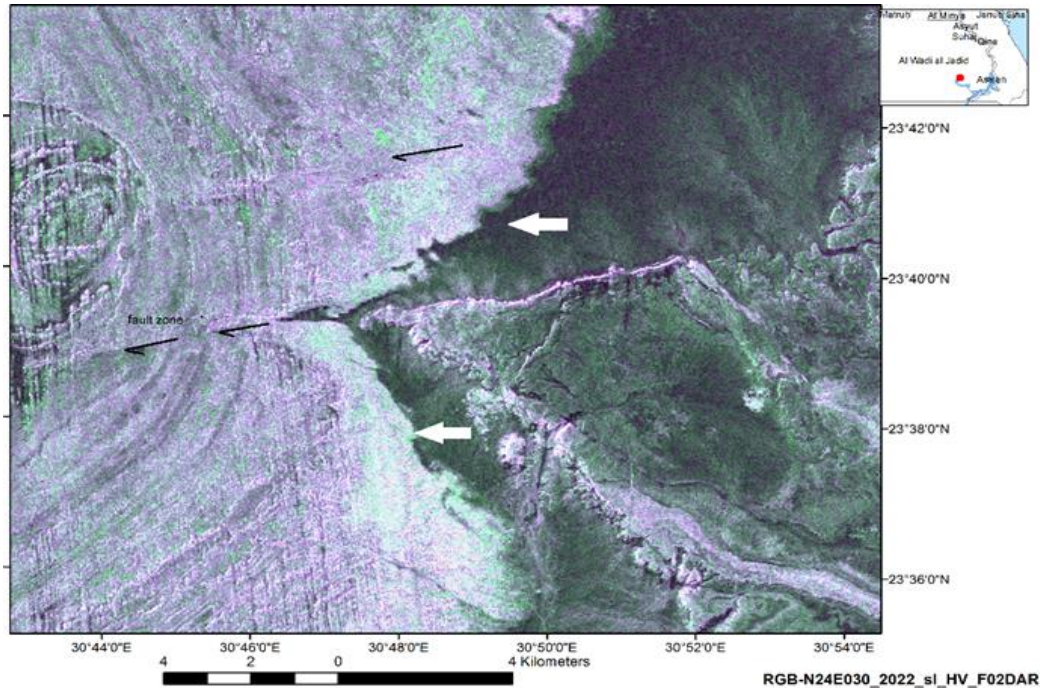

Figure 10: ALOS PALSAR radar scene two separating blocks with congruent margins.

Figure 11 shows nearly the same area in a perspective view with a height exaggeration (20 x) to visualize the probable rifting (white arrows).

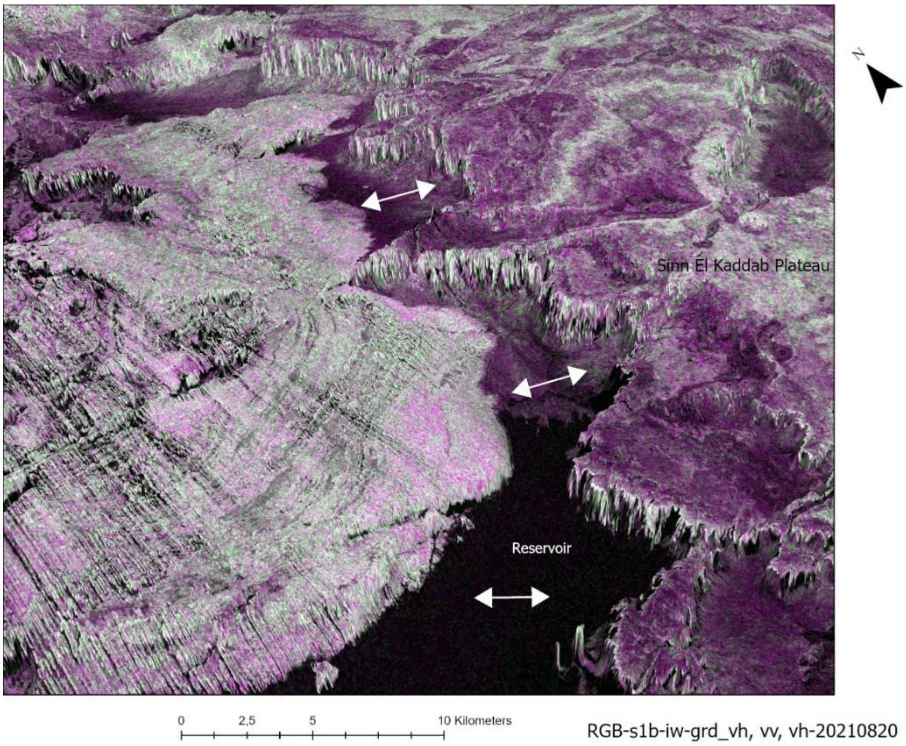

Figure 11: Rift valley development (?) in a perspective 3D view of a Sentinel 1 radar scene with 20 x height exaggeration. The southern part is flooded by the reservoir.

The reservoir flooding in the southern part of the valley might trigger rifting processes as surface water intrudes into the probably deep reaching fault zones. The increase of water pore pressure and poroelastic stress can decrease the effective strength of the rock beneath the reservoir; the fluids making slip along existing faults under stress more likely.

Topographic cross sections reveal distinct escarpments with height differences of about 100 m and steep slopes along the assumed take-off zones along the eastern valley margins (Figure 12). This topographic setting might support the assumption that the steep escarpments correspond to take-off zones, where the rifting process started. However, to verify the rifting processes geologic and geophysical field work such the elaboration of 3D seismic profiles, and geodetic measurements would be necessary. In the northern part of the investigation area, in the eastern rim of the Kargha valley, the height differences amount up to 300 m with the consequence of intense morphodynamic processes (slope failure, strong erosion and sedimentation).

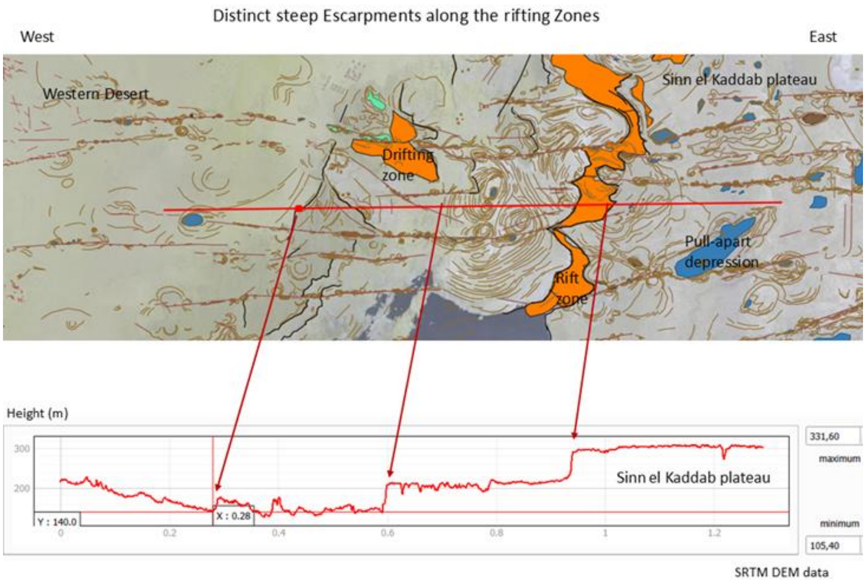

Figure 12: Topographic E-W- cross section passing probable rift valleys indicating distinct escarpments along the eastern valley margins.

Like the circular and oval-shaped structures the probable rift valleys are situated in the same belt of geodynamic activities (Figure 13). The "belt" of rotation structures and probable rift valleys shows the same orientation as many dikes striking SSW-NNE in the Western Desert (dark-red lines on Figure 13) in the west of Sinn El Kaddab plateau following the Nubian fault systems, thus, tracing deep seated zones of weakness.

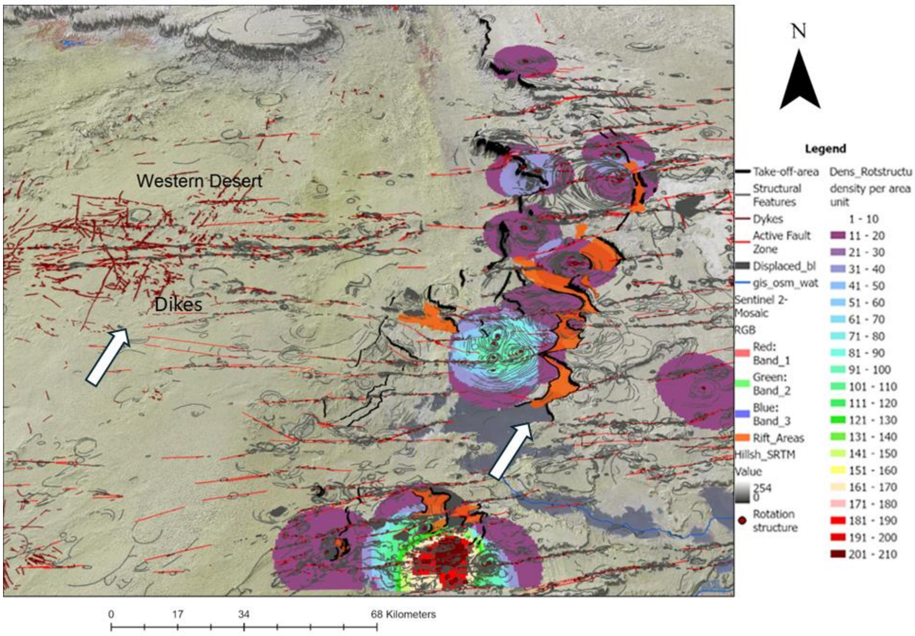

Figure 13: 3D perspective view of the SSW-NNE oriented "belt" of circular structures, their density calculation and probable rift valleys. The rift zones show the same main orientation as dikes in the western desert following weak zones in the subsurface.

D. Traces of block movements and Slope failure

Another indicator for geodynamic activities is the occurrence of block movements. Satellite images support their detection and the tracing of their movements. This is demonstrated by the next Figures 14, 15 and 16, presenting examples of lithologic units that have been obviously dislocated. Figure 14 displays a Sentinel 1 radar scene of an area where displaced block movements appear obviously.

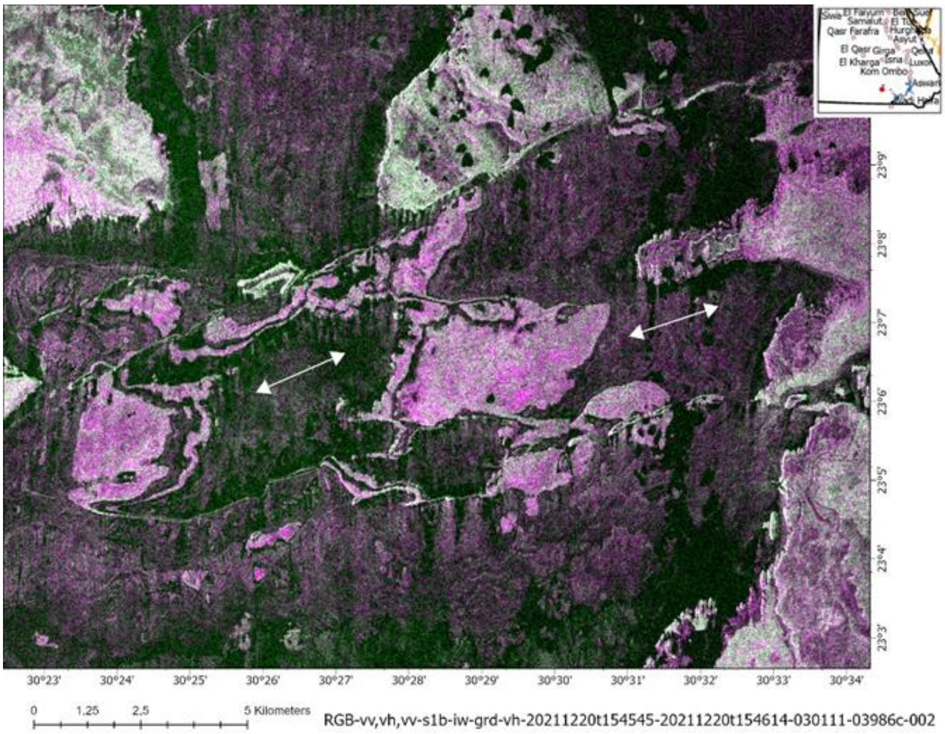

Figure 14: Sentinel 1 radar scene of dislocated blocks (pink) in the SW of the Sinn el Kaddab plateau. The white arrows visualize the movements along active fault zones over several kilometers.

The same area is visible on Figure 15 using the thermal bands of Landsat and ASTER images.

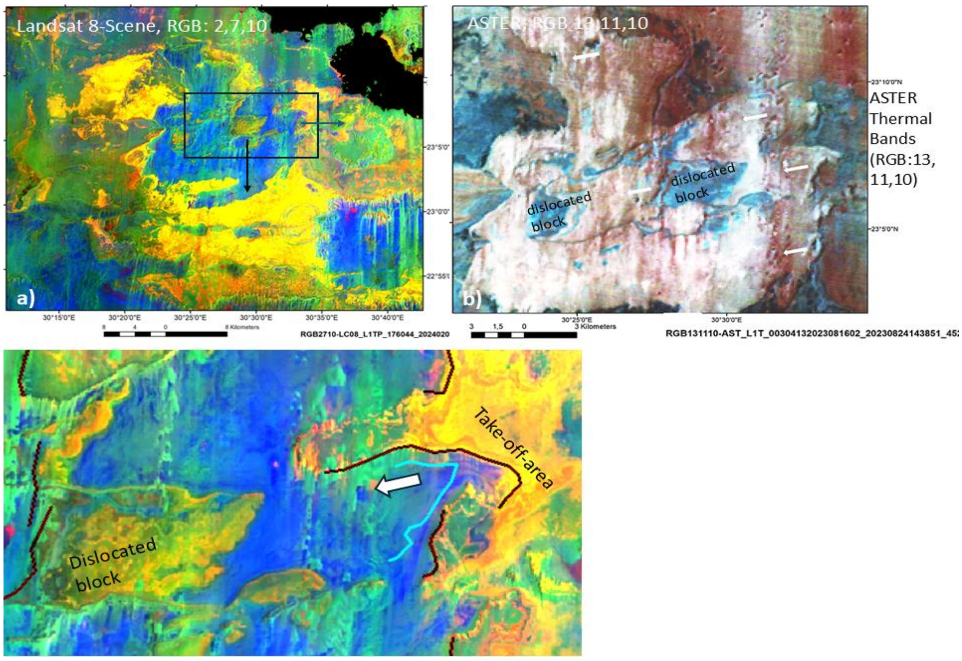

Figure 15: Traces of block movements on a) Landsat (RGB, bands: 2,7,10) and b) ASTER (RGB, bands: 13,11,10) images including thermal bands. The ASTER image is showing obviously dislocated blocks in blue colors. The contours of the blocks match in their outline and shape with the outline of the take-off zones in the east.

The probable rotation structures in limestones and marls of the Sinn el Kaddab plateau are predominantly circular or oval-shaped, and appear more or less to be situated "in situ" without a prominent dislocation of the affected rocks over distances. The dislocated blocks, however, seem to have been moved up to kilometers. The shapes and contours of dislocated blocks in the Western Desert change according to their specific lithologic and structural setting. Some of the obviously dislocated blocks in the Western Desert in the SW of the Sinn el Kaddab plateau show a more "ear-shaped" outline as if broken apart. They appear as single, dislocated (allochthon) blocks. Examples of these types of rotation and drifting structures are presented in the next figures (Figures 16 and 17). Whether this outline is related to the lithologic conditions, tectonic stress, intensities and / or velocities of movements along the active fault zones, or intersecting of fault zones, has still to be investigated.

As demonstrated by Figures 16 and 17 the combination and joint evaluation of different satellite images provides more information than the use of only one data source. The focus on a specific type of satellite data has to be adapted to the environmental circumstances. The structural information is mainly based on radar images as aeolian covers prevent or restrict their visibility on optical satellite images. ALOS PALSAR L-Band signal penetration of loose sediments are estimated to reach up to 2 m [33] (Mansour et al.2024).

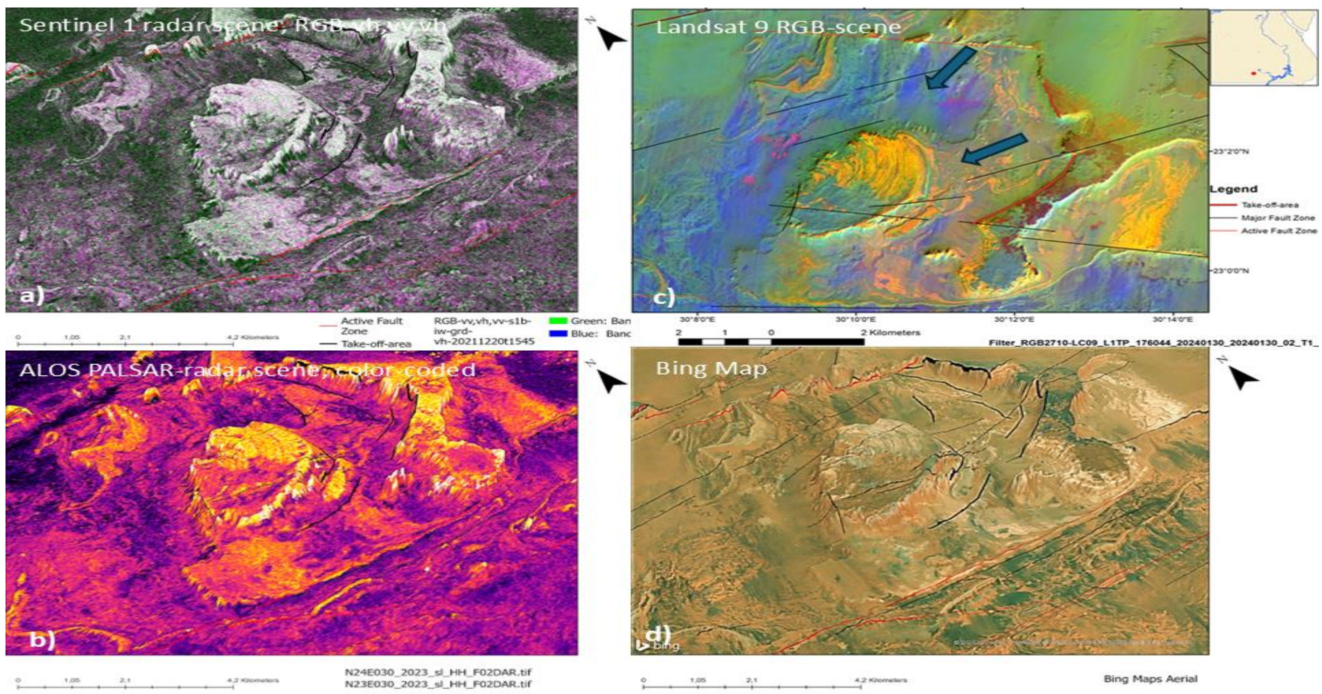

Figure 16: "Ear-shaped" dislocated blocks visible on different satellite images: a) Sentinel 1, b) color-coded ALOS PALSAR, c) Landsat, and d) Bing Map. The blue arrows indicate the moving direction of the block.

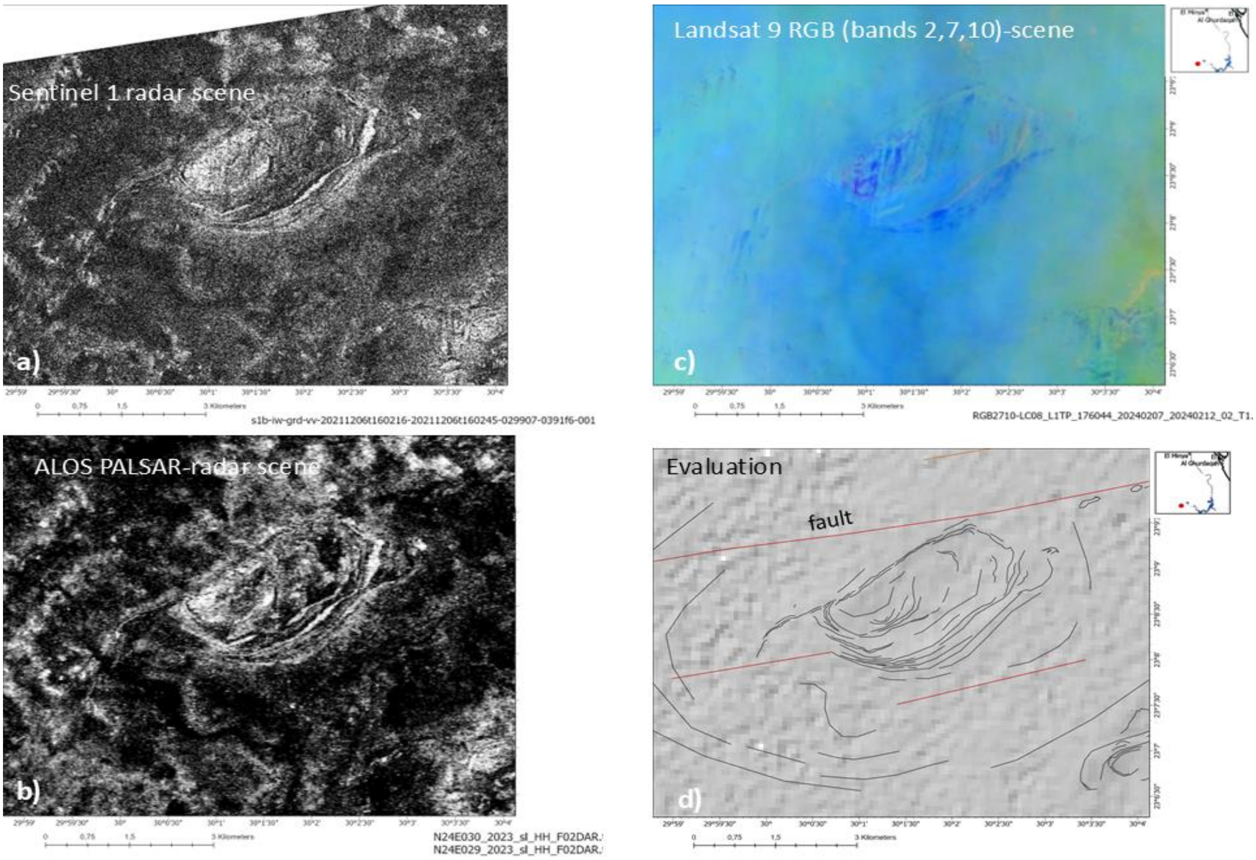

Figure 17: Drifting block visible on radar images (a and b), and a Landsat scene (c).

The next examples show large, elongated blocks oriented in WNW-ESE direction that seem to be dislocated as well. However, whether these are just larger push-up-ridges along active fault zones or just dislocated parts of rock units, this has to be investigated in the field. An indicator for the dislocation and movements of these single blocks/ ridges towards west might be the height difference along the steeper slopes of the assumed take-off areas. In Fig.17 a height level map is presented indicating in red colors the lower areas in front of the steeper slopes that could be caused by mass deficits related to the block movements. Normally a gradual height level decrease at the foot plains could be expected.

The same area is shown on the Sentinel 1-radar scene (Figure 19). Areas of displacements forming depressions in the back of moving blocks might be interesting for groundwater exploration. In combination of large, active fault zones with relatively higher permeability for groundwater flow these depressions could be affected by rainwater infiltration more than the environment, even with the very rare rain events in this desert climate. Locally, the El-Kharga Oasis receives less than 0.1 mm/year of precipitation and lacks naturally occurring surface water [34]. Water management and irrigation as visible on Figure 19, especially its planning, is a complex task that includes the awareness of active geodynamic processes, to avoid damage to the irrigation systems. Due to high consumption rates and overexploitation, the groundwater level in the northern half of the Kharga Oasis declined from 60 to 80 m below the earth and from 40 to 60 m in the southern part between 1967 and 2007 [34]. Radar and Landsat image evaluations might support the detection of surface and groundwater flow (Figure 20).

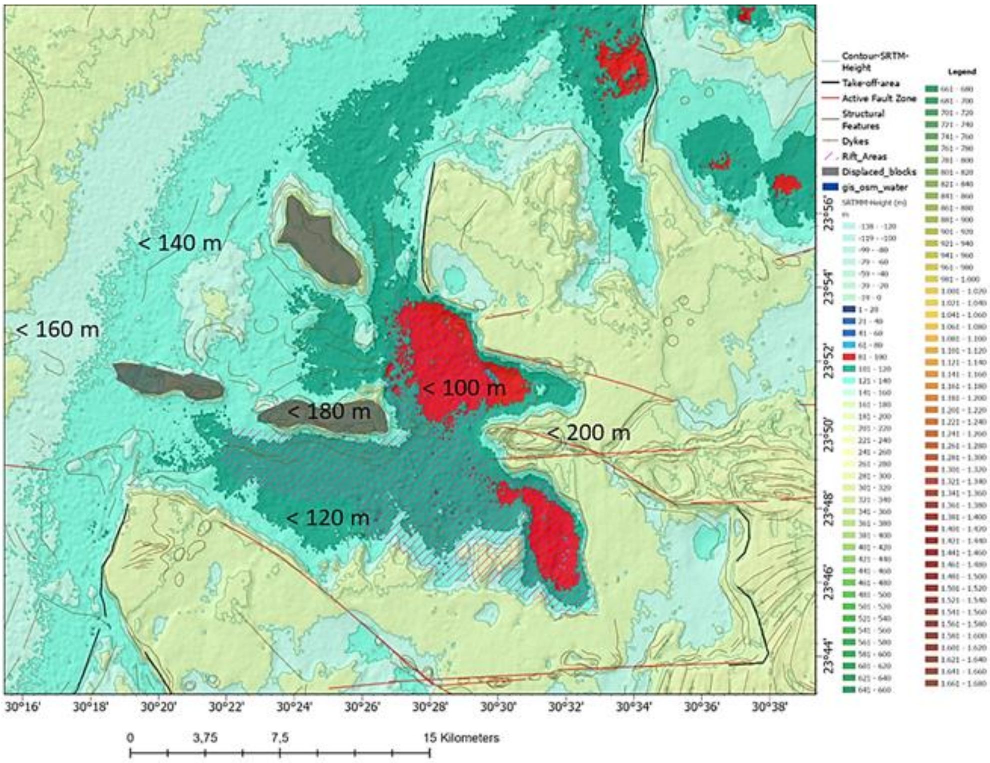

Figure 18: Height level map indicating in red (< 100 m) and dark-green (< 120 m) areas assumed to show mass deficits because of block drifting (blocks: dark-gray).

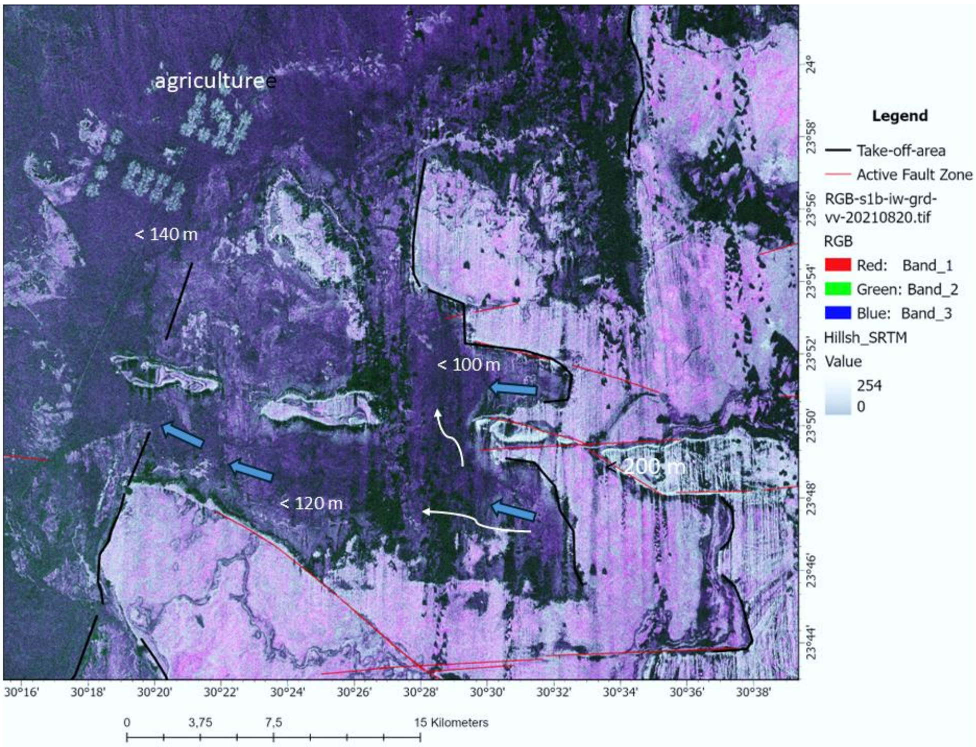

Figure 19: Sentinel 1-radar scene (RGB, created based on the different polarizations: vh.vv,vh).

Slope failure and mass movements along the cliffs are another indicator for geodynamic activity in the Kharga valley and southern adjacent areas. The occurrence, size and intensity of slope failures along the eastern border of the Kharga valley might be influenced by uplifting of the Sinn el Kaddab plateau described by [35] and by the intersection of active fault zones perpendicular to the N-S and SSW-NNE oriented cliffs. Rifting processes might be another explanation.

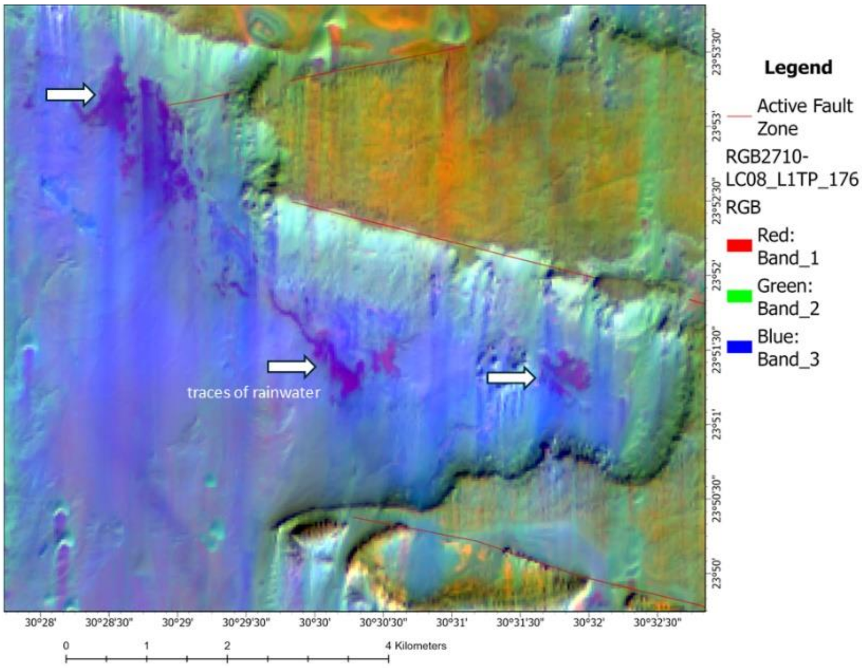

Figure 20: Landsat 8 scene including the thermal bands 7 and 10 in an RGB image showing dark-blue-violet areas in the depressions where surface water infiltrated, that might be of interest for groundwater exploration.

The next Figure 21 shows an example of slope instability along the western border of the Sinn El Kaddab-plateau. The western cliffs are obviously prone to block gliding and rock fall. The example presents an area where the front cliff of the western border of the Sinn el Kaddab plateau was already separated from a large, elongated block. The separation is indicated by the congruent, "zipper-like" outline of the eastern rim of the block and the western rim of the cliff.

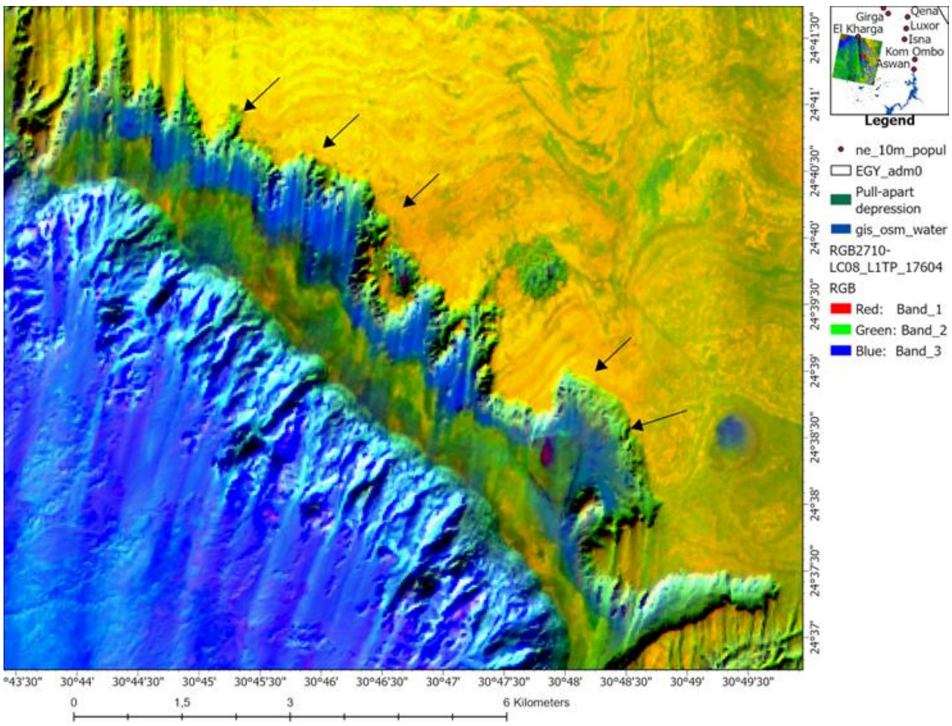

Figure 21: Rupture and down-gliding of a dislocated front-block of about 10 km length and 1 km width at the western border of the Sinn el Kaddab-Plateau moving downwards towards SW.

The next figure (Figure 22) comprises 3D perspective views of this separated front-block to visualize the geologic and geomorphologic situation. Shales and marls in this area are susceptible to mass movements along the steep slopes. Traces of active faults with pull-apart depression and push-up-ridges are visible on the different satellite images as well, bordering in the north and south of the separated block. Their dynamics might have had an influences on the block-gliding.

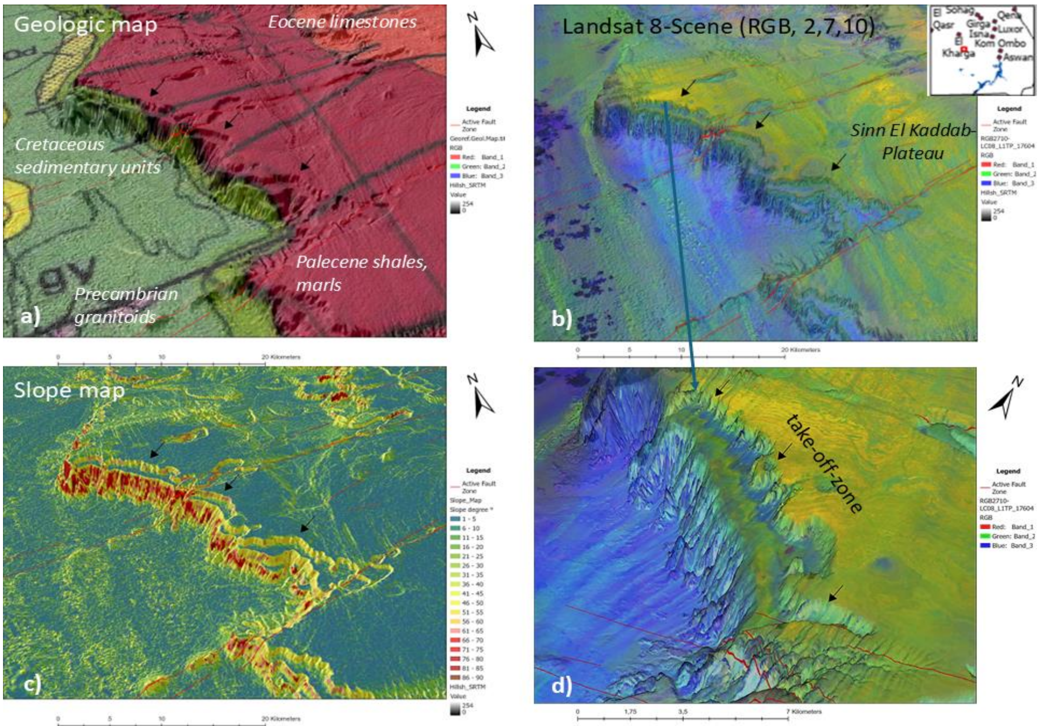

Figure 22: 3D perspective views of the area of the separated front-block showing a) the geologic setting [36], b and d) Landsat 8 perspective views, and with 20 x height exaggeration (SRTM DEM), c) the slope degrees. Red lines indicate active fault zones.

The southern fault zone of the elongated, dislocated block seems not to have only an impact on cliff stability, but also on groundwater flow as several oases are aligned along this fault zone (Figure 23).

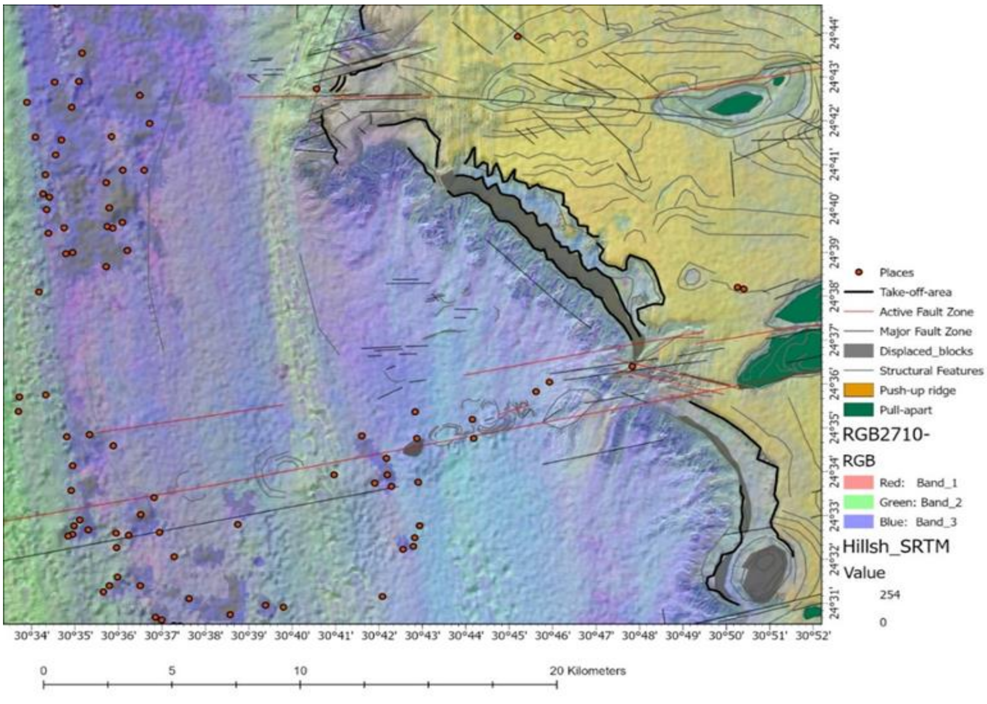

Figure 23: Settlements (red points) with available wells aligned along a WSW-ENE striking active fault zone intersecting the western part of the Sinn el Kaddab plateau and its western border visible on a Landsat scene. Faults generally are the most permeable zones for groundwater flow.

As the limestones in the Sinn el Kaddab plateau have been affected by intense tectonic stress (due to uplifting, movements along active fault zones or rotation) during the geologic past, the rock units have been fractured and dislocated. The nowadays rare rainwater from the higher areas in the Sinn el Kaddab plateau infiltrate into these fracture and fault zones and into a complex underground conduit system within the lime-and dolostones (with typical karst hydrogeologic properties) and, following the hydraulic gradient, is obviously flowing towards west into the Kharga valley (Figure 24). Groundwater and surface water exchange with both adjacent and distant aquifers through underground channels can be expected. The tectonic / geodynamic situation is affecting the groundwater setting in this area such as by influencing the development of the karst hydrogeologic network, the hydraulic gradient and the permeability of the rocks.

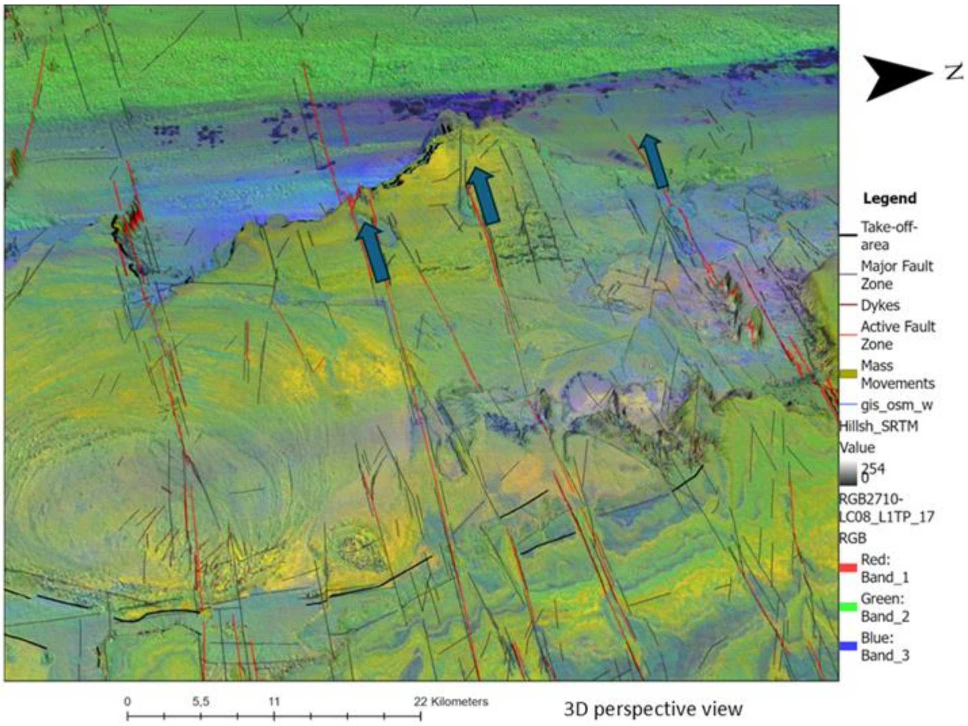

Figure 24: 3D perspective Landsat view looking towards west into the Kharga valley with irrigation agriculture (visible in dark-blue colors). The blue arrows visualize the groundwater flow direction within the active fault zones with a relatively higher water permeability.

Figure 25 provides an overview of the areas prone to slope failure and block displacements as far as it could be detected on the high resolution satellite images.

Along the western cliffs of the Sinn el Kaddab plateau slope failures (block gliding, rock fall) are a distinct phenomenon and more pronounced than along the eastern border. Whether they are recent or they are paleo-landslides, or both, and reactivated, this cannot be determined based on remotes sensing data. Field work is necessary to solve this. Nevertheless, block displacements and mass movements can be used as indicators for neotectonic activities when observed and documented continuously and combined with geodetic measurements.

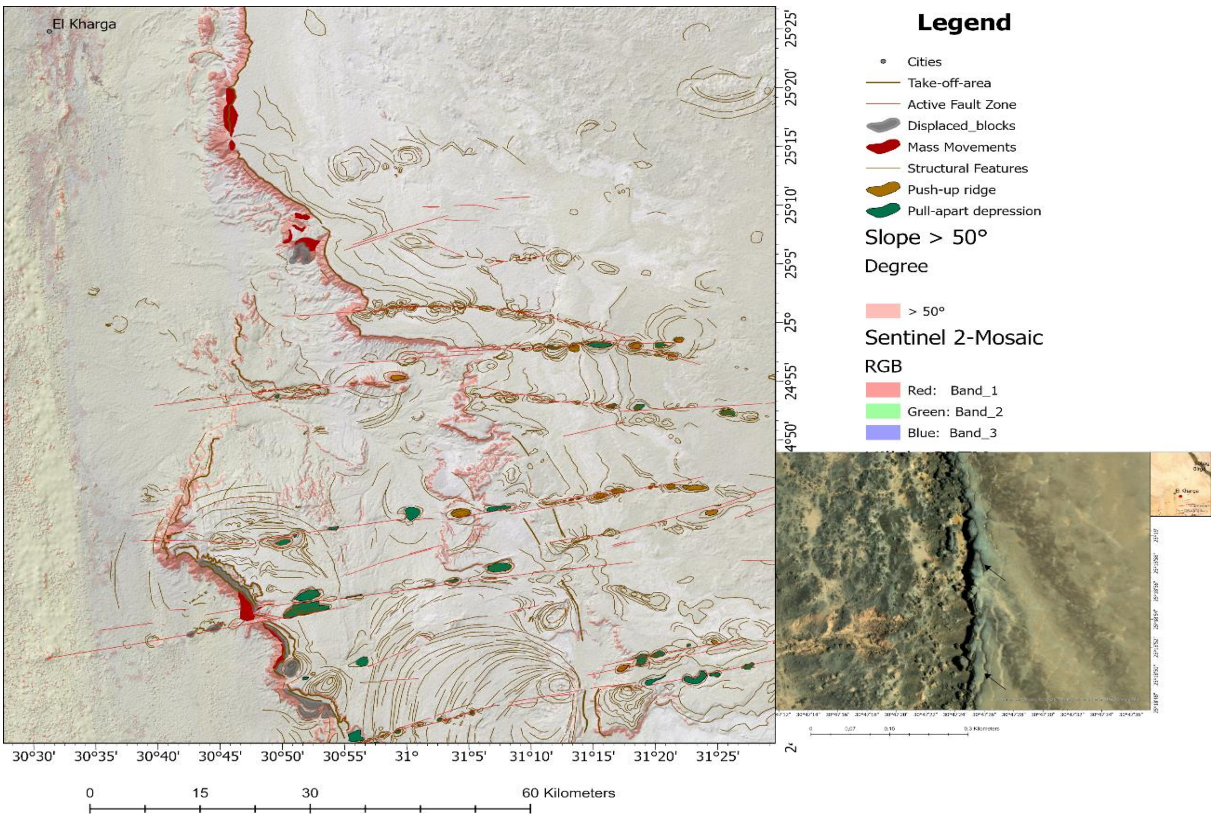

Figure 25: Overview of areas prone to slope failure.

F. Morphometric Analysis

DEM data have proven to be a valuable tool for neotectonic investigations as demonstrated by the following Figure 26. Although the “Fill sink” algorithm from the ArcGIS Pro software was originally developed to fill all sinks / depressions in the DEM generated from data errors (spurious artifacts), they reveal as well real, subtle topographic features. The difference raster between the sink-filled (“depressionless” DEM) and original DEM data set highlights different types of depressions such as pull-apart basins along active fault zones. The resulting raster map visualizes those areas where the differences of the subtraction of (Fill sinks SRTM-DEM) minus (original SRTM-DEM) occur concentrated. This approach has been tested with ASTER DEM data as well with superimposing results.

When using SRTM and ASTER DEM data to get the difference map after carrying out the Fill-sink function in ArcGIS Pro based on the original DEM, there is a match of the areas with the highest difference values and the area assumed to be prone to rifting processes (Figure 26). The areas with the highest difference values coincide as well with the position of thermal well and hot springs. Hot spring reach the Earth’s surface through weak zones. Rift systems are generally the most promising tectonic setting for the development of hot springs [4]. These places have tectonic regimes that are characterized by extension. This creates fractures and fault networks that allow geothermally heated water to move upward [37]. Additionally, areas with higher permeability, such as cracked basement rocks that make it simple for geothermal fluids to circulate, are frequently associated with hot springs. The geological structures such as fault systems and permeable rock units, form pathways for the movement of fluids from deep underground [25].

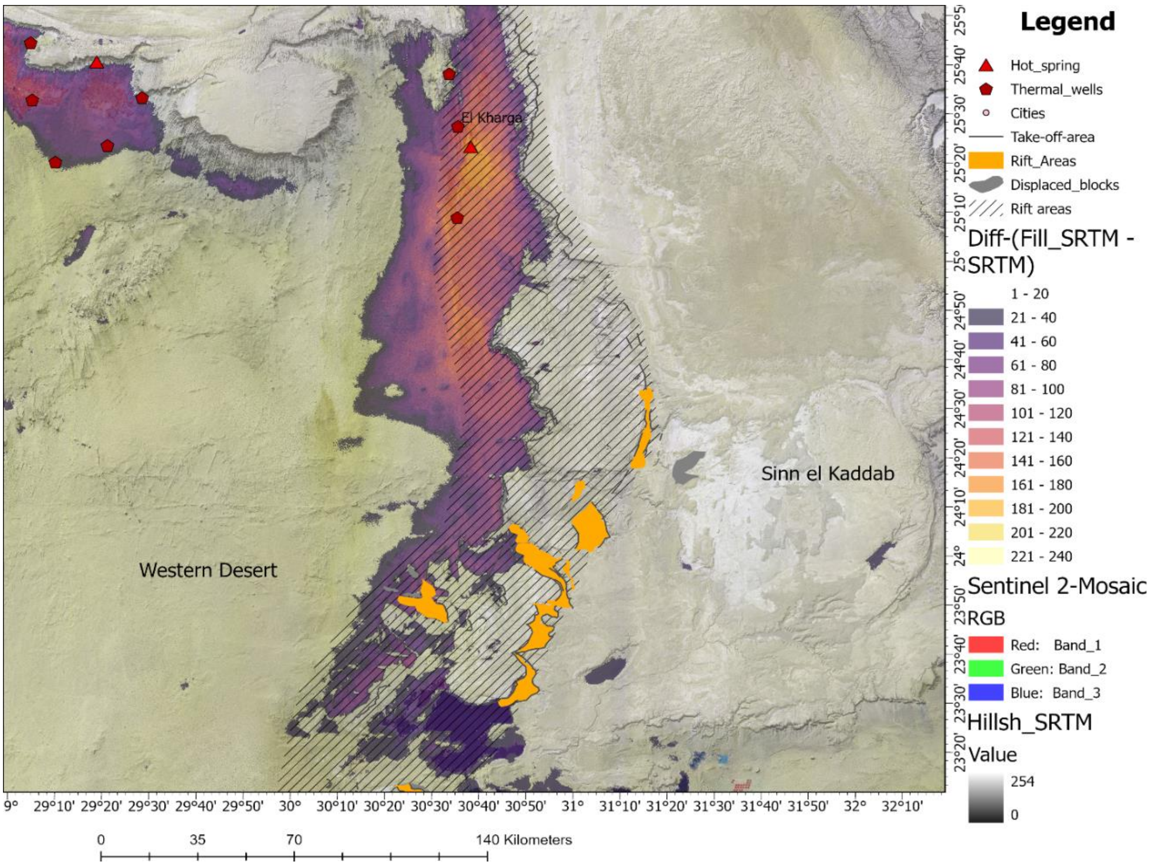

Figure 26: Difference raster between the sink-filled (“depressionless” DEM) and original DEM data set (Fill-SRTM – SRTM DEM) highlighting concentrations of differences.

G. Integration of geophysical Data

The evaluation results of remote sensing data were combined with geophysical data. When integrating earthquake data into the GIS it becomes obvious that there is no remarkable earthquake activity in the area (Figure 27). Most of the earthquakes in the investigation area happened in depths below 10 km. However, little is known about aseismic, gliding movements.

It was investigated whether heat flow maps can provide further information. Heat flow is the movement of heat (or energy) from the interior of the Earth to the surface. Units: mW / m2 (milliwatts per metre squared). The conductive surface heat flow (qs), also termed terrestrial heat flow, provides insight into the steady-state thermal situation of an area for time scales of tens of millions of years. Deep-rooted magmatic processes linked with rifting and plume generation caused lithosphere thinning and upwelling of the asthenospheric mantle. Terrestrial heat flow data help to understand the underground temperature patterns, in spite of insufficient data coverage [24][25].

There are sparse observations from temperature gradient measurements in Egypt. The heat flow values provided by the International Heat Flow Commission (IHFC) within the investigation area increase from south towards north from above 20 to 100 mW / m2 (Figure 28). The Dakhla and Kharga Oases are featured by hot springs and thermal wells with surface temperatures up to 50°C.

Remote sensing was used as well to observe land surface temperatures. Higher positive thermal anomalies could be detected on Sentinel-3 LST images acquired in 2019 and confirmed using the 2020 LST images of Egypt. One of seven thermal anomalies in Egypt is covering the Kharga area [4].

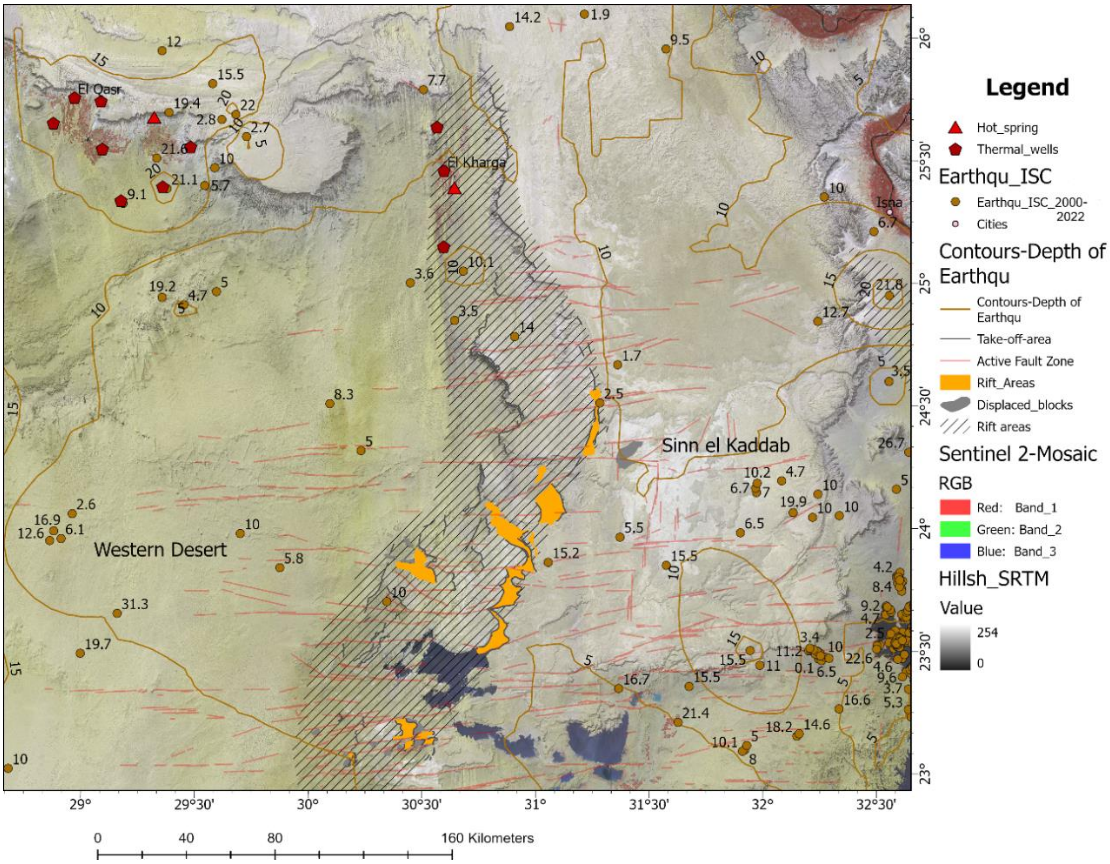

Figure 27: Earthquake occurrence and their depth (km).

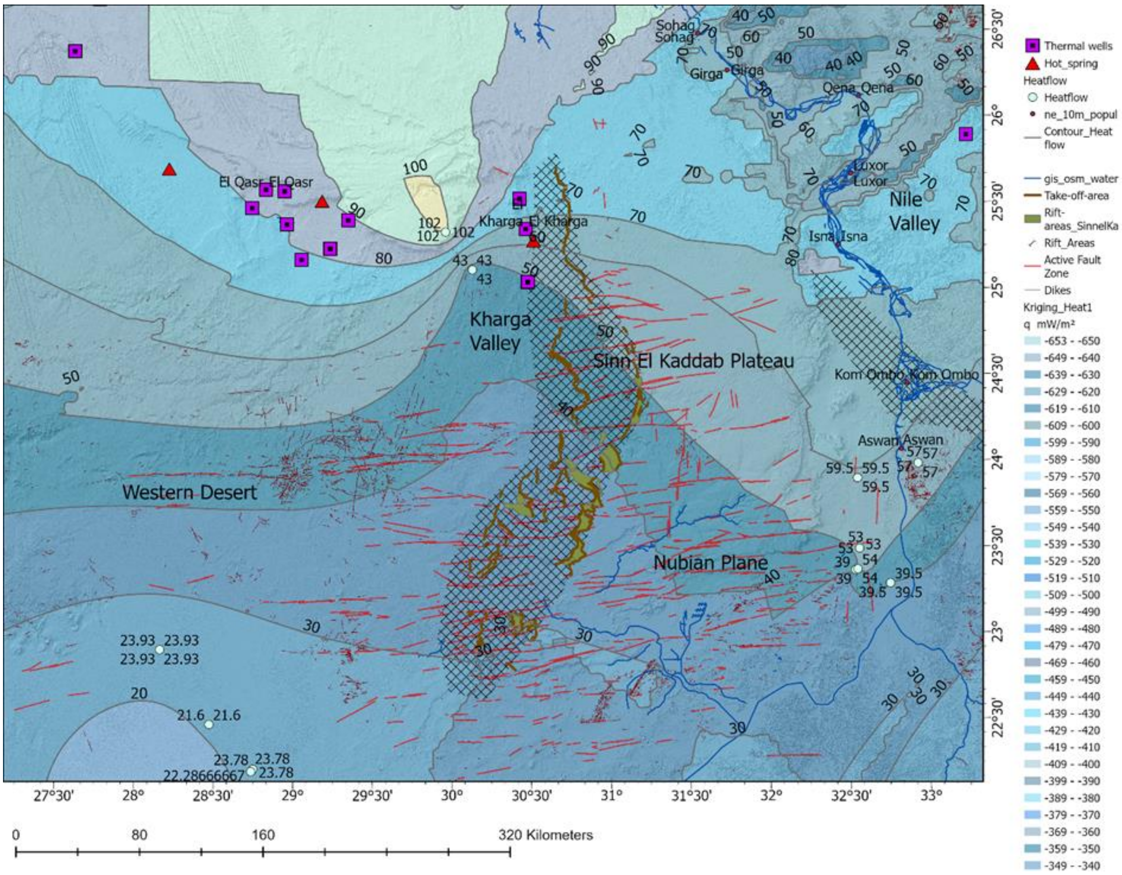

Figure 28: Heat flow map of the investigation area based on IASPEI data [23], Kriging interpolated.

As further geophysical data set Bouguer gravity [38] and aeromagnetic data were used as well as available geological data to gain more reliable information about structures in the investigation area. The gravity field gives an integrated response to density contrasts caused by structural features on regional and local scales. The higher mass of the crust causes in generally positive gravity anomalies [22]. The contours of the Bouguer anomalies reveal anomalies striking SSW-NNE in the southern part and N-S in the northern part with values of 90 -110 m Gal. The anomaly contours match in their position and shape the contours of the areas with traces of rifting and block drifting.

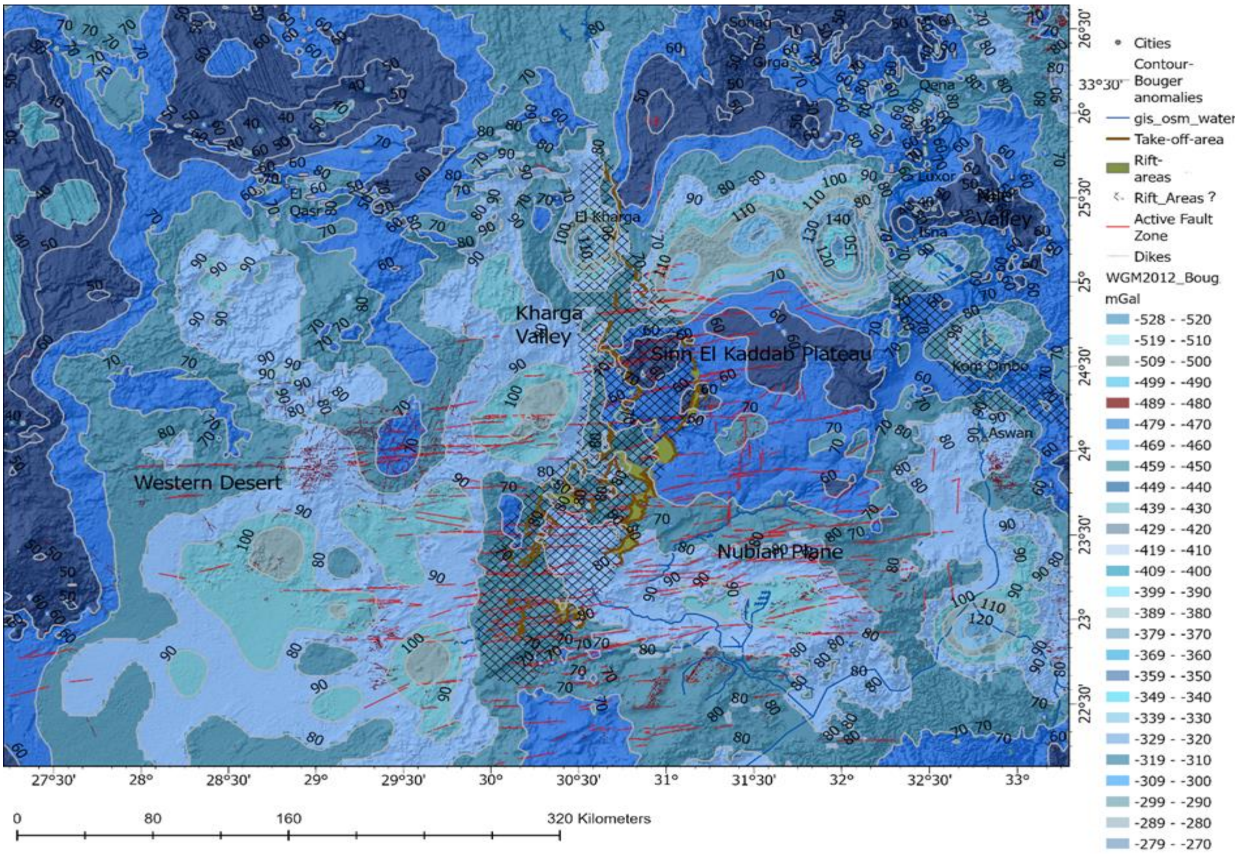

Figure 28: Bouguer-gravity map based on WGM2012_Bouguer_ponc_2min.grd-data [38].

Crustal properties related information can be derived from the CPD map of this area derived from aeromagnetic data as shown in Figure 29. (The Curie point depth, CPD, is the depth in the Earth's crust at which ferromagnetic minerals are converted into para-magnetic minerals due to an increase in the temperature.) Airborne magnetic data were extracted from the grid of AMMP (Africa Magnetic Mapping Project). The AMMP final products contain 1 km digital grid of total field crustal anomalies. The shallowest CPDs are associated with crustal thinning [37].

In the west of the Sinn el Kaddab Plateau the areas with the lowest (from the surface point of view) CPD depth values (> 26 km, dark-blue on the lower map in Figure 29 b) correspond to the lowest topographic regions at the surface (< 120 m, dark-green in Fig.29 a). The lowest area below 120 m height level are forming depressions like the Kharga oasis valley in SSW-NNE direction and are partly matching with the assumed rifting area Whether there is a geodynamic relationship like subsidence or rifting between the lower CPD depth position and the lower surface topography, this has still to be investigated. Underneath the Sinn El Kaddab Plateau the CPD depth was estimated to be in less than 20 km. Uplifting movements in the Sinn el Kaddab Plateau were described by [35]. These uplifting movements could have intensified faulting and block-wise rotations at its borders.

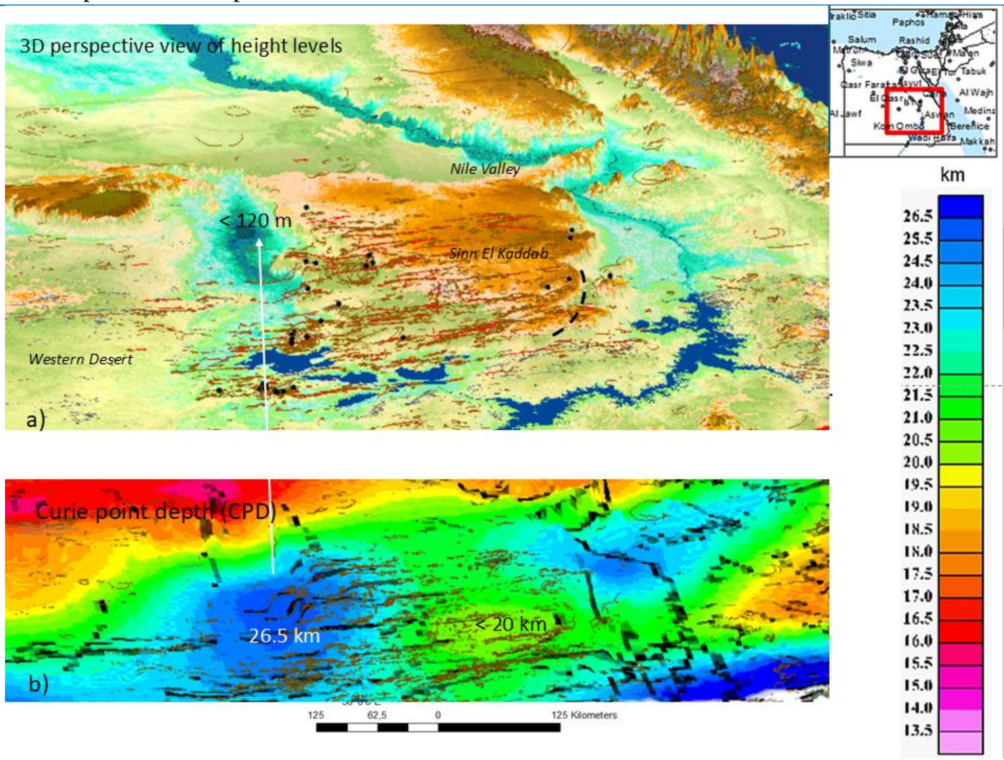

Figure 29: Combining topographic data with CPD information. (a) 3D perspective view of the height level map (above, looking north) and the Curie Point Depth (CPD) map. The CPD-map was created by [37] [39] Structure lines, derived from the geological map [36], overprinted on the map [39].

5. Conclusions

It is of particular interest to identify and characterize long-term mechanically weak regions in Egypt as they are areas with a high potential for tectonic reworking at different scales. Neotectonic investigations comprising remote sensing, and geospatial analysis have become efficient tools to identify the active tectonic spots, uplift or slip rates on the active faults in the investigation area [10] [40] [41] [42]. When merging the different layers in a GIS environment it becomes obvious that observed traces of geodynamic movements occur concentrated in a SSW-NNE oriented "belt" bordering the Sinn el Kaddab plateau that nearly match with geophysical indicators such as Bouguer gravity anomalies or with CPD contours.

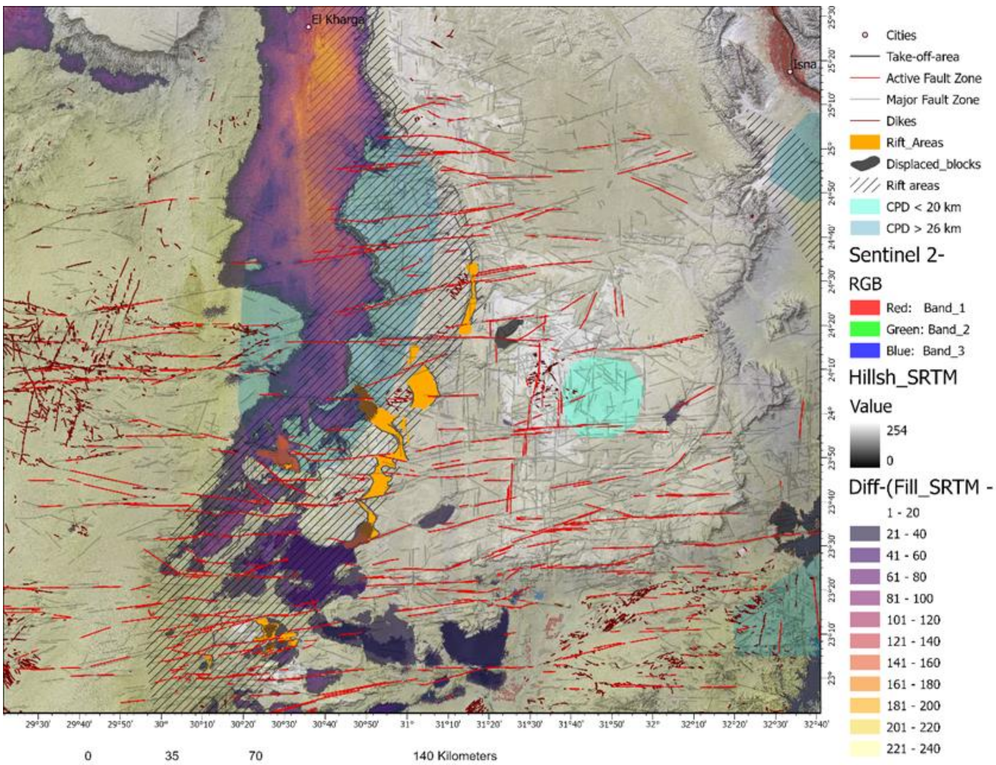

Figure 30: Overlay of the SRTM derived DEM difference map with CPD depths.

Several indicators that might contribute to a better understanding of the structural / tectonic situation, especially in rifting areas in Central Egypt, were investigated using remote sensing and GIS tools. By combining different information layers about active faults, the structural pattern, displacement of rock units, slope failure and further geological and geophysical data in a GIS data base, an overview of the main structures could be achieved. The concentration of dislocated and drifting blocks, circular and oval-shaped features, congruent valley rims in rift zones, slope failure, etc. in a SSW-NNE oriented "belt" in the west and southwest of the Sinn el Kaddab plateau and the eastern part of the Kharga valley, leads to the conclusion that this belt displays intense neotectonic activity. Whether this is related to larger-scaled rifting processes has still to be investigated. Geodetic and more detailed geophysical data are needed to clarify the character of the movements.

Acknowledgment
The author thanks the team of the Journal of Earth & Environment Science for their support.

References

1. A. Abdelkhalek, "Late Paleogene - Early Neogene Abandoned Rift along the River Nile, Egypt," Dissertation zur Erlangung des mathematisch-naturwissenschaftlichen Doktorgrades "Doctor rerum naturalium" der Georg-August-Universität Göttingen im Promotionsprogramm Geowissenschaften, Georg-August University School of Science (GAUSS), Abteilung Strukturgeologie und Geodynamik, Geowissenschaftliches Zentrum, Georg-August-Universität, Göttingen, 2020.
2. A. Mostafa, A. El-Barkooky, and M. Hammed, "Structural geometry and tectonic evolution of an Early Cretaceous rift crossing the Nile Valley in Upper Egypt," Basin Research.;vol. 34,pp.1731–1762. 2022. https://doi.org/10.1016/j.marpetgeo.2023.106289
3. M. Ali, M. Y. Ali, A. Abdelhady, and J. D. Fairhead, "Tectonic evolution and subsidence history of the Cretaceous basins in southern Egypt: The Komombo Basin," Basin Research, vol. 34, pp.1731–1762, 2022, DOI: 10.1111/bre.12683
4. A. A. Madani and S. M. Said, "Satellite land surface temperature for mapping the structurally controlled geothermal anomalies in the Cretaceous rift, South Egypt," NRIAG Journal of Astronomy and Geophysics, vol. 13,1, pp. 141-152, 2024, DOI:10.1080/20909977.2024.2381383, https://doi.org/10.1080/20909977.2024.2381383.
5. S. Saleh, "The role of geophysical and seismological data in evaluating the subsurface structures and tectonic trends of Nile Delta, Egypt," Arab J Geosci, vol. 6, pp.3201–3216, 2013. DOI 10.1007/s12517-012-0603-9
6. W. Bosworth, S. M. Khalil, M. Ligi, D. F. Stockli, and K. R. McClay, "Geology of Egypt: The Northern Red Sea," In: Z. Hamimi, A. El-Barkooky, J. M. Frías, H. Fritz, and Y. Abd El-Rahman (Editors)," The Geology of Egypt," Chapter 9, pp. 344-369, 2020. https://doi.org/10.1007/978-3-030-15265-9
7. A. Delaunay, G. Baby, J. Fedorik, A. M. Afifi, P. Tapponnier, and J. Dyment, "Structure and morphology of the Red Sea, from the mid-ocean ridge to the ocean-continent boundary," Tectonophysics, vol. 849, 229728, 2023, https://doi.org/10.1016/j.tecto.2023.229728
8. B. Tewksbury, C.J. Mehrtens, S.A. Gohlke, E.A. Tarabees, and J.P Hogan, "Constraints from Mesozoic siliciclastic cover rocks and satellite image analysis on the slip history of regional E-W faults in the southeast Western Desert," Egypt. J. Afr. Earth Sci., vol. 136, pp. 119–135, 2017. http://dx.doi.org/10.1016/j.jafrearsci.2017.06.026
9. B. Theilen-Willige, "Remote Sensing for neotectonic Investigations: A Case Study from Southern Egypt," in: M. Gupta (Editor), "Remote Sensing for Geophysicists," Chapter 10, pp.141-164, 2025, 1. edition, CRC Press, Taylor and Francis Group, FL, USA, DOI: 10.1201/9781003485278-13, https://doi.org/10.1201/9781003485
10. B. Theilen-Willige, A. Hamed, M. Khalifa, and A. Abdelgowad, "Remote Sensing Applications comprising geological and geophysical Data for neotectonic Investigations: A Case Study in South-Central-Egypt," Mediterranean Journal of Basic and Applied Sciences (MJBAS), vol. 9, 1, pp. 109-141, January-March 2025. https://doi.org/10.46382/MJBAS.2025.9108
11. B. Theilen-Willige, "Overview of Fault Zones based on Remote Sensing Data as Contribution to the Safety of Infrastructure and Land Use in Southern Egypt," Prevention and Treatment of Natural Disasters, vol. 3, 1, pp. 17-50, 2024. https://doi.org/10.54963/ptnd.v3i1.227
12. W. Cavazza, T. Gusmeo, M. Zattin, V. Alania, O. Enukidze, S. Corrado, and A. Schito, "Two-step exhumation of Caucasian intraplate rifts: A proxy of sequential plate-margin collisional orogenies," Geoscience Frontiers, 15 (2024) 101737, 2024. https://doi.org/10.1016/j.gsf.2023.101737
13. A. K. Shah, T. L. Pratt, and J. W. Horton, "Rift Basins and Intraplate Earthquakes: New High-Resolution Aeromagnetic Data Provide Insights Into Buried Structures of the Charleston, South Carolina Seismic Zone," Geochemistry, Geophysics, Geosystems, vol. 24, e2022GC010803, 2023. https://doi.org/10.1029/2022GC010803
14. A. Abdelhalim, E. Abuelella, S. Sakran, and S. M. Said, "Implementation of Space-Borne Optical Data and Field Investigation for Geo-structural Mapping of an Interior Rift Basin: A Case Study from Kharit Area, Southeastern Desert, Egypt," Journal of Mining and Environment (JME), vol. 14, 4, pp. 1037-1059, 2023. DOI: 10.22044/jme.2023.12739.2327
15. E. Zelenin, D. Bachmanov, S. Garipova, V. Trifonov, and A. Kozhurin, " The Active Faults of Eurasia Database (AFEAD): the ontology and design behind the continental-scale dataset," Earth Syst. Sci. Data, vol. 14, pp. 4489–4503, 2022. https://doi.org/10.5194/essd-14-4489-2022
16. Arab Nubia Group Blog, GIS, Remote Sensing & General, Applications. Available online: https://blog.arabnubia.com/
17. A. K. Abdel-Fattah, M. Fnais, M. F. Abdelwahed, A. El-Nekhely, and W. Farid, " Fault orientations in the upper crust beneath an intraplate active zone in northern Egypt," Earth Planets Space, vol. 65, pp. 739–748, 2013. doi:10.5047/eps.2012.12.005
18. US Geological Survey (USGS), Earth Explorer, https://earthexplorer.usgs.gov/.
19. European Space Agency (ESA), Copernicus Browser. https://dataspace.copernicus.eu/browser/
20. NASA Earth Data, Alaska Satellite Facility (ASF). https://search.asf.alaska.edu/#/

21. Japan Aerospace Exploration Agency, Earth Observation Research Center (JAXA EORC), PALSAR-2 Global Forest/ Non-forest Map "2023". https://www.eorc.jaxa.jp/alos/en/palsar_fnf/data/2023/map.htm
22. I.S. Ismail, S. A. Saada, Y. M.Y. Ali, and Y. M.Y. Ibrahem (2015), “An Integrated Study of Gravity and Magnetic Data to Determine Subsurface Structure and Depth to Basement in Alamein Area, Western Desert, Egypt,” IOSR Journal of Applied Geology and Geophysics, (IOSR-JAGG) e-ISSN: 2321–0990, p-ISSN 2321–0982,vol. 3, 6, Ver.II, pp. 11-29, Nov. - Dec. 2015. DOI: 10.9790/0990-03621129.
23. International Heat Flow Commission, Global Heat Flow Data Assessment Group: S.Fuchs, F. Neumann, et.al., “The Global Heat Flow Database: Release 2024,” GFZ Data Services. 2024. https://doi.org/10.5880/fidgeo.2024.014
24. A. M. Bekhit, M. Sobh, M. A. Zaher, T. A. Fattah, and A. I. Diab, “Predicting terrestrial heat flow in Egypt using random forest regression: a machine learning approach,” Geothermal Energy, vol. 13, 18, 2025. https://doi.org/10.1186/s40517-025-00341-w.
25. A. M. Bekhit, M. Sobh, M. A. Zaher, T. A. Fattah, and A. I. Diab, “Crustal thickness variations beneath Egypt through gravity inversion and forward modeling: linking surface thermal anomalies and Moho topography,” Progress in Earth and Planetary Science (2024), vol. 11, https://doi.org/10.1186/s40645-024-00639-6
26. USGS, Search Earthquake Catalog. https://earthquake.usgs.gov/earthquakes/search/
27. EMSC Euro-Mediterranean Seismological Centre (EMSC), earthquake data. http://www.emsc-csem.org/.
28. International Seismological Centre (ISC), ISC Bulletin: event catalogue search. http://www.isc.ac.uk/iscbulletin/search/bulletin/interactiv/
29. A. Mostafa, A. El-Barkooky, M. Hammed, “Structural geometry and tectonic evolution of an Early Cretaceous rift crossing the Nile Valley in Upper Egypt,” Basin Research. 2022, vol. 34, pp. 1731–1762, 2023. https://doi.org/10.1016/j.marpetgeo.2023.106289
30. H.A. Alrefaee, “Crustal modeling of the central part of the Northern Western Desert, Egypt using gravity data,” J. Afr. Earth Sci., vol. 129, pp. 72–81, 2017. https://doi.org/10.1016/j.jafrearsci.2016.12.012
31. M. Rashwan, R. Sawires, A.M. Radwan, F. Sparacino, J.A. Peláez, and M. Palano, “Crustal Strain and Stress Fields in Egypt from Geodetic and Seismological Data,” Remote Sens., vol. 13, 1398, 2021. https://doi.org/10.3390/rs13071398
32. S. Sakran, S.M.Said, “Structural Setting and Kinematics of Nubian Fault System, SE Western Desert, Egypt: An Example of Multi-Reactivated Intraplate Strike-Slip Faults,” Journal of Structural Geology, vol. 107, pp. 93-108, 2018. https://doi.org/10.1016/j.jsg.2017.12.006
33. K. Mansour, M. A. Zaher, M. Al Deep, N. Medhat, S. Ebrahim, and A. Mohamed, “Validation of ALOS/PALSAR Subsurface Penetration Depth in Farafra Oasis as an Arid Region Based on Field Ground-Penetrating Radar Measurements,” Sensing and Imaging, vol. 25:21, 2024. https://doi.org/10.1007/s11220-024-00472-7
34. M. Saber, M. Mokhtar, A. Bakheit, A. M. Elfeky, M. Gameh, A. Mostafa, A. Sefelnasr, S. A. Kantoush, T. Sumi, T. Hori, and A. Hamada, “An integrated assessment approach for fossil groundwater quality and crop water requirements in the El-Kharga Oasis, Western Desert, Egypt,” Journal of Hydrology: Regional Studies, vol. 40, 101016, 2022. https:// doi.org/ 10.1016/j.ejrh.2022.101016
35. K.A. Elmagd, M.W. Ali-Bik, and A. Emam, “Geomorphic Evolution of The Kurkur-Dungul area in Response to Tectonic Uplifting and Climatic Changes, South Western Desert, Egypt,” International Journal of Civil & Environmental Engineering IJCEE-IJENS, vol. 15, 01, 157801-6565-IJECS-IJENS, February 2015.
36. Egyptian Geological Survey and Mining Authority, “Geologic Map of Egypt, “1: 2 Mio, Cairo, Egypt, 1981. https://esdac.jrc.ec.europa.eu/content/geologic-map-egypt
37. M.A. Zaher, S. Elbarbary, A. El-Shahat, H. Mesbah, and A. Embaby, “Geothermal resources in Egypt integrated with GIS based analysis,” J. Volcanol. Geotherm. Res., vol. 365, pp. 1–12, 2018. doi:10.1016/j.jvolgeores.2018.09.013
38. S. Bonvalot, A. Briais, M. Kuhn, A. Peyrefitte, N. Vales, R. Biancale, G. Gabalda, G. Moreaux, F. Reinquin, and M. Sarrailh, “Global grids: World Gravity Map (WGM2012),” Bureau Gravimetrique International, 2012. https://doi.org/10.18168/bgi.23
39. M.A. Zaher, and S. Elbarbary, “Investigation of Geothermal Resources in Egypt Using Geophysical Data,” Proceedings World Geothermal Congress, 2020+1, Reykjavik, Iceland, April - October 2021, https://www.researchgate.net/publication/351785852_Investigation of_Geothermal_Resources_in_Egypt_Using_Geophysical_Data.
40. A. Khalifa, B. Bashir, A. Alsalman, and Nazik Ögretmen, “Morpho-Tectonic Assessment of the Abu-Dabbab Area, Eastern Desert, Egypt: Insights from Remote Sensing and Geospatial Analysis, “ISPRS Int. J.Geo-Inf. 2021, 10, 784. https://doi.org/10.3390/ijgi10110784
41. M. K. Alawy, J. Gomez-Barreiro, Z. Hamimi, A.K. M. Moghazi, M. H. Younis, I.Puente Orench, S. B. S´anchez, “Tectonic reworking in the Arabian-Nubian Shield: An analysis of thetextural record of the exhumation of the Meatiq Gneiss dome (Egypt),” Gondwana Research, vol. 143, pp. 64–90, 2025. https://doi.org/10.1016/j.gr.2025.03.008
42. E. L. Heckenbach, S. Brune, A. C. Glerum, R. Granot, Y. Hamiel, S. V. Sobolev, D.Neuharth“ 3D Interaction of Tectonics and Surface Processes Explains Fault Network Evolution of the Dead Sea Fault,” TEKTONIKA, vol. 2.2, pp. 33-51, 2024. https://tektonika.online/index.php/home/article/view/75